

1 **The evolution of root zone moisture capacities after**
2 **deforestation: a step towards hydrological predictions**
3 **under change?**

4

5 **Remko Nijzink¹, Christopher Hutton², Ilias Pechlivanidis⁴, René Capell⁴, Berit**
6 **Arheimer⁴, Jim Freer^{2,3}, Dawei Han², Thorsten Wagener^{2,3}, Kevin McGuire⁵,**
7 **Hubert Savenije¹, Markus Hrachowitz¹**

8 [1] Water Resources Section, Faculty of Civil Engineering and Geosciences, Delft University
9 of Technology, Stevinweg 1, 2628 CN Delft, The Netherlands

10 [2] Department of Civil Engineering, University of Bristol, Bristol, UK

11 [3] Cabot Institute, University of Bristol, BS8 1UJ, Bristol, UK

12 [4] Swedish Meteorological and Hydrological Institute (SMHI), Norrköping, Sweden

13 [5] Virginia Water Resources Research Center and Department of Forest Resources and
14 Environmental Conservation, Virginia Tech, Blacksburg, VA, USA

15 Correspondence to: R. C. Nijzink (r.c.nijzink@tudelft.nl)

16

17

1 **Abstract**

2 The core component of many hydrological systems, the moisture storage capacity available to
3 vegetation, is impossible to observe directly at the catchment scale and is typically treated as a
4 calibration parameter or obtained from a priori available soil characteristics combined with
5 estimates of rooting depth. Often this parameter is considered to remain constant in time.
6 Using long-term data (30-40 years) from three experimental catchments that underwent
7 significant land cover change, we tested the hypotheses that: (1) the root zone storage capacity
8 significantly changes after deforestation, (2) changes in the root zone storage capacity can to a
9 large extent explain post-treatment changes to the hydrological regimes and that (3) a time-
10 dynamic formulation of the root zone storage can improve the performance of a hydrological
11 model.

12 A recently introduced method to estimate catchment-scale root zone storage capacities based
13 on climate data (i.e. observed rainfall and an estimate of transpiration) was used to reproduce
14 the temporal evolution of root zone storage capacity under change. Briefly, the maximum
15 deficit that arises from the difference between cumulative daily precipitation and transpiration
16 can be considered as a proxy for root zone storage capacity. This value was compared to the
17 value obtained from four different conceptual hydrological models that were calibrated for
18 consecutive 2-year windows.

19 It was found that water-balance derived root zone storage capacities were similar to the values
20 obtained from calibration of the hydrological models. A sharp decline in root zone storage
21 capacity was observed after deforestation, followed by a gradual recovery, for two of the three
22 catchments. Trend analysis suggested hydrological recovery periods between 5 and 13 years
23 after deforestation. In a proof-of-concept analysis, one of the hydrological models was
24 adapted to allow dynamically changing root zone storage capacities, following the observed
25 changes due to deforestation. Although the overall performance of the modified model did not
26 considerably change, in 51% of all the evaluated hydrological signatures, considering all three
27 catchments, improvements were observed when adding a time-variant representation of the
28 root zone storage to the model.

29 In summary, it is shown that root zone moisture storage capacities can be highly affected by
30 deforestation and climatic influences and that a simple method exclusively based on climate-
31 data can not only provide robust, catchment-scale estimates of this critical parameter, but also
32 reflect its time-dynamic behavior after deforestation.

1 **1 Introduction**

2 Vegetation as a core component of the water cycle, shapes the partitioning of water fluxes on
3 the catchment scale into runoff components and evaporation, thereby controlling fundamental
4 processes in ecosystem functioning (Rodriguez-Iturbe, 2000; Laio et al., 2001; Kleidon,
5 2004), such as flood generation (Donohue et al., 2012), drought dynamics (Seneviratne et
6 al., 2010; Teuling et al., 2013), groundwater recharge (Allison et al., 1990; Jobbágy and
7 Jackson, 2004) and land-atmosphere feedback (Milly and Dunne, 1994; Seneviratne et al.,
8 2013; Cassiani et al., 2015). Besides increasing interception storage available for evaporation
9 (Gerrits et al., 2010), vegetation critically interacts with the hydrological system in a co-
10 evolutionary way by root water uptake for transpiration, towards a dynamic equilibrium with
11 the available soil moisture to avoid water shortage (Donohue et al., 2007; Eagleson, 1978,
12 1982; Gentine et al., 2012; Liancourt et al., 2012) and related adverse effects on carbon
13 exchange and assimilation rates (Porporato et al., 2004; Seneviratne et al., 2010). Roots create
14 moisture storage volumes within their range of influence, from which they extract water that
15 is stored between field capacity and wilting point. This root zone storage capacity S_R ,
16 sometimes also referred to as plant available water holding capacity, in the unsaturated soil is
17 therefore the key component of many hydrological systems (Milly and Dunne, 1994;
18 Rodriguez-Iturbe et al., 2007).

19 There is increasing theoretical and experimental evidence that vegetation dynamically adapts
20 its root system, and thus S_R , to environmental conditions, to secure, on the one hand, access
21 to sufficient moisture to meet the canopy water demand and, on the other hand, to minimize
22 the carbon investment for sub-surface growth and maintenance of the root system (Brunner et
23 al., 2015; Schymanski et al., 2008; Tron et al., 2015). In other words, the hydrologically
24 active root zone is optimized to guarantee productivity and transpiration of vegetation, given
25 the climatic circumstances (Kleidon, 2004). Several studies previously showed the strong
26 influence of climate on this hydrologically active root zone (e.g. Reynolds et al., 2000; Laio et
27 al., 2001; Schenk and Jackson, 2002). Moreover, droughts are often identified as critical
28 situations that can affect ecosystem functioning evolution (e.g. Allen et al., 2010; McDowell
29 et al., 2008; Vose et al.).

30 In addition to the general adaption to environmental conditions, vegetation has some potential
31 to adapt roots to such periods of water shortage (Sperry et al., 2002; Mencuccini, 2003; Bréda
32 et al., 2006). In the short term, stomatal closure and reduction of leaf area will lead to reduced

1 transpiration. In several case studies for specific plants, it was also shown that plants may
2 even shrink their roots and reduce soil-root conductivity during droughts, while recovering
3 after re-wetting (Nobel and Cui, 1992; North and Nobel, 1992). In the longer term, and more
4 importantly, trees can improve their internal hydraulic system, for example by recovering
5 damaged xylem or by allocating more biomass for roots (Sperry et al., 2002; Rood et al.,
6 2003; Bréda et al., 2006). Similarly, Tron et al. (2015) argued that roots follow groundwater
7 fluctuations, which may lead to increased rooting depths when water tables drop. Such
8 changing environmental conditions may also provide other plant species with different water
9 demand, than the ones present under given conditions, with an advantage in the competition
10 for resources, as for example shown by Li et al. (2007).

11 The hydrological functioning of catchments (Black, 1997; Wagener et al., 2007) and thus the
12 partitioning of water into evaporative fluxes and runoff components is not only affected by
13 the continuous adaption of vegetation to changing climatic conditions. Rather, it is well
14 understood that anthropogenic changes to land cover, such as deforestation, can considerably
15 alter hydrological regimes. This has been shown historically through many paired watershed
16 studies (e.g. Bosch and Hewlett, 1982; Andréassian, 2004; Brown et al., 2005; Alila et al.,
17 2009). These studies found that deforestation often leads to generally higher seasonal flows
18 and/or an increased frequency of high flows in streams, while decreasing evaporative fluxes.
19 The time scales of hydrological recovery after such land cover disturbances were shown to be
20 highly sensitive to climatic conditions and the growth dynamics of the regenerating species
21 (e.g. Jones and Post, 2004; Brown et al., 2005) .

22 Although land-use change effects on hydrological functioning are widely acknowledged, it is
23 less well understood, which parts of the hydrological system are affected in which way and
24 over which time scales. As a consequence, most catchment-scale models were originally not
25 developed to deal with such changes in the system, but rather for ‘stationary’ conditions
26 (Ehret et al., 2014). This is true for both top-down hydrological models, such as HBV
27 (Bergström, 1992) or GR4J (Perrin et al., 2003), and bottom-up models, such as MIKE-SHE
28 (Refsgaard and Storm, 1995) or HydroGeoSphere (Brunner and Simmons, 2012). Several
29 modelling studies have in the past incorporated temporal effects of land use change to some
30 degree (Andersson and Arheimer, 2001; Bathurst et al., 2004; Brath et al., 2006), but they
31 mostly rely on ad hoc assumptions about how hydrological parameters are affected (Legesse
32 et al., 2003; Mahe et al., 2005; Onstad and Jamieson, 1970; Fenicia et al., 2009). Approaches

1 which incorporate the change in the model formulation itself, are rare and have only recently
2 gained momentum (e.g. Du et al., 2016; Faticchi et al., 2016; Zhang et al., 2016). This is of
3 critical importance as on-going land cover and climate change dictates the need for a better
4 understanding of their effects on hydrological functioning (Troch et al., 2015) and their
5 explicit consideration in hydrological models for more reliable predictions under change
6 (Hrachowitz et al., 2013; Montanari et al., 2013).

7 As a step towards such an improved understanding and the development of time-dynamic
8 models, we argue that the root zone storage capacity S_R , is a core component determining the
9 hydrological response, and needs to be treated as dynamically evolving parameter in
10 hydrological modelling as a function of climate and vegetation. Gao et al. (2014) recently
11 demonstrated that catchment-scale S_R can be robustly estimated exclusively based on long-
12 term water balance considerations. Wang-Erlansson et al. (2016) derived global estimates of
13 S_R using remote-sensing based precipitation and evaporation products, which demonstrated
14 considerable spatial variability of S_R in response to climatic drivers. In traditional approaches,
15 S_R is typically determined either by the calibration of a hydrological model (e.g. Seibert and
16 McDonnell, 2010; Seibert et al., 2010) or based on soil characteristics and sparse, averaged
17 estimates of root depths, often obtained from literature (e.g. Breuer et al., 2003; Ivanov et al.,
18 2008). This does neither reflect the dynamic nature of the root system nor does it consider to a
19 sufficient extent the actual function of the root zone: providing plants with continuous and
20 efficient access to water. This leads to the situation that soil porosity often effectively
21 controls the values of S_R used in a model. Consider, as a thought experiment, two plants of the
22 same species growing on different soils. They will, with the same average root depth, then
23 have access to different volumes of water, which will merely reflect the differences in soil
24 porosity. This is in strong contradiction to the expectation that these plants would design root
25 systems that provide access to similar water volumes, given the evidence for efficient carbon
26 investment in root growth (Milly, 1994; Schymanski et al., 2008; Troch et al., 2009) and
27 posing that plants of the same species have common limits of operation. This argument is
28 supported by a recent study, in which was shown that water balance derived estimates of S_R
29 are at least as plausible as soil derived estimates (de Boer-Euser et al., 2016) in many
30 environments and that the maximum root depth controls evaporative fluxes and drainage
31 (Camporese et al., 2015).

1 Therefore, using water balance based estimates of S_R in several deforested as well as in
2 untreated reference sites in two experimental forests, we test the hypotheses that (1) the root
3 zone storage capacity S_R significantly changes after deforestation, (2) the evolution in S_R can
4 explain post-treatment changes to the hydrological regimes and that (3) a time-dynamic
5 formulation of S_R can improve the performance of a hydrological model.

6

7 **2 Study sites**

8 The catchments under consideration are part of the H.J. Andrews Experimental Forest and the
9 Hubbard Brook Experimental Forest. A summary of the main catchment characteristics can
10 be found in Table 1. Daily discharge (Campbell, 2014a; Johnson and Rothacher, 2016),
11 precipitation (Campbell, 2014b; Daly and McKee, 2016) and temperature time series
12 (Campbell, 2014c, 2014d; Daly and McKee, 2016) were obtained from the databases of the
13 Hubbard Brook Experimental Forest and the HJ Andrews Experimental Forest. Potential
14 evaporation was estimated by the Hargreaves equation (Hargreaves and Samani, 1985).

15 **2.1 H.J. Andrews Experimental Forest**

16 The H.J. Andrews Experimental Forest is located in Oregon, USA (44.2°N , 122.2°W) and
17 was established in 1948. The catchments at H.J. Andrews are described in many studies (e.g.
18 Rothacher, 1965; Dyrness, 1969; Harr et al., 1975; Jones and Grant, 1996; Waichler et al.,
19 2005).

20 Before vegetation removal and at lower elevations the forest generally consisted of 100- to
21 500-year old coniferous species, such as Douglas-fir (*Pseudotsuga menziesii*), western
22 hemlock (*Tsuga heterophylla*) and western redcedar (*Thuja plicata*), whereas upper elevations
23 were characterized by noble fir (*Abies procera*), Pacific silver fir (*Abies amabilis*), Douglas-
24 fir, and western hemlock. Most of the precipitation falls from November to April (about 80%
25 of the annual precipitation), whereas the summers are generally drier, leading to signals of
26 precipitation and potential evaporation that are out of phase..

27 Deforestation of H.J. Andrews WS1 started in August 1962 (Rothacher, 1970). Most of the
28 timber was removed with skyline yarding. After finishing the logging in October 1966, the
29 remaining debris was burned and the site was left for natural regrowth. WS2 is the reference
30 catchment, which was not harvested.

1 **2.2 Hubbard Brook Experimental Forest**

2 The Hubbard Brook Experimental Forest is a research site established in 1955 and located in
3 New Hampshire, USA (43.9°N, 71.8°W). The Hubbard Brook experimental catchments are
4 described in a many publications (e.g. Hornbeck et al., 1970; Hornbeck, 1973; Dahlgren and
5 Driscoll, 1994; Hornbeck et al., 1997; Likens, 2013).

6 Prior to vegetation removal, the forest was dominated by northern hardwood forest composed
7 of sugar maple (*Acer saccharum*), American beech (*Fagus grandifolia*) and yellow birch
8 (*Betula alleghaniensis*) with conifer species such as red spruce (*Picea rubens*) and balsam fir
9 (*Abies balsamea*) occurring at higher elevations and on steeper slopes with shallow soils. The
10 forest was selectively harvested from 1870 to 1920, damaged by a hurricane in 1938, and is
11 currently not accumulating biomass (Campbell et al., 2013; Likens, 2013). The annual
12 precipitation and runoff is less than in H.J. Andrews (Table 1). Precipitation is rather
13 uniformly spread throughout the year without distinct dry and wet periods, but with snowmelt
14 dominated peak flows occurring around April and distinct low-flows during the summer
15 months due to increased evaporation rates (Federer et al., 1990). Vegetation removal occurred
16 in the catchment of WS2 between 1965-1968 and in WS5 between 1983-1984. Hubbard
17 Brook WS3 is the undisturbed reference catchment.

18 Hubbard Brook WS2 was completely deforested in November and December 1965 (Likens et
19 al., 1970). To minimize disturbance, no roads were constructed and all timber was left in the
20 catchment. On June 23, 1966, herbicides were sprayed from a helicopter to prevent regrowth.
21 Additional herbicides were sprayed in the summers of 1967 and 1968 from the ground.

22 In Hubbard Brook WS5, all trees were removed between October 18, 1983 and May 21, 1984,
23 except for a 2 ha buffer near an adjacent reference catchment (Hornbeck et al., 1997). WS5
24 was harvested as a whole-tree mechanical clearcut with removal of 93% of the above-ground
25 biomass (Hornbeck et al., 1997; Martin et al., 2000); thus, including smaller branches and
26 debris. Approximately 12% of the catchment area was developed as the skid trail network.
27 Afterwards, no treatment was applied and the site was left for regrowth.

1 **3 Methodology**

2 To assure reproducibility and repeatability, the executional steps in the experiment were
 3 defined in a detailed protocol, following Ceola et al. (2015), which is provided as
 4 supplementary material in Section S1.

5 **3.1 Water balance-derived root zone moisture capacities S_R**

6 The root zone moisture storage capacities S_R and their change over time were determined
 7 according to the methods suggested by Gao et al. (2014) and subsequently successfully tested
 8 by de Boer-Euser et al. (2016) and Wang-Erlundsson et al. (2016). Briefly, the long-term
 9 water balance provides information on actual mean transpiration. In a first step, the
 10 interception capacity has to be assumed, in order to determine the effective precipitation P_e [L
 11 T^{-1}], following the water balance equation for interception storage:

$$12 \quad \frac{dS_i}{dt} = P - E_i - P_e \quad , \quad (1)$$

13 With S_i [L] interception storage, P the precipitation [$L T^{-1}$], E_i the interception evaporation [L
 14 T^{-1}]. This is solved with the constitutive relations:

$$15 \quad 16 \quad E_i = \begin{cases} E_p & \text{if } E_p dt < S_i \\ \frac{S_i}{dt} & \text{if } E_p dt \geq S_i \end{cases} \quad (2)$$

$$17 \quad P_e = \begin{cases} 0 & \text{if } S_i \leq I_{max} \\ \frac{S_i - I_{max}}{dt} & \text{if } S_i > I_{max} \end{cases} \quad (3)$$

18 With, additionally, E_p the potential evaporation [$L T^{-1}$] and I_{max} [L] the interception capacity.
 19 As I_{max} will also be affected by land cover change, this was addressed by introducing the three
 20 parameters $I_{max,eq}$ (long-term equilibrium interception capacity) [L], $I_{max,change}$ (post-treatment
 21 interception capacity) [L] and T_r (recovery time) [T], leading to a time-dynamic formulation
 22 of I_{max} :

$$I_{max} = \begin{cases} I_{max,eq} & \text{for } t < t_{change}, t > t_{change,end} + T_r \\ I_{max,eq} - \frac{I_{max,eq} - I_{max,change}}{t_{change,end} - t_{change,start}} (t - t_{change,start}) & \text{for } t_{change,start} < t < t_{change,end} \\ I_{max,change} + \frac{I_{max,eq} - I_{max,change}}{T_r} (t - t_{change,end}) & \text{for } t_{change,end} < t < t_{change,end} + T_r \end{cases} \quad (4)$$

2 with $t_{change,start}$ the time that deforestation started and $t_{start,end}$ the time deforestation finished.

3 Following a Monte-Carlo sampling approach, upper and lower bounds of E_i were then
4 estimated based on 1000 random samples of these parameters, eventually leading to upper and
5 lower bounds for P_e . The interception capacity was assumed to increase after deforestation for
6 Hubbard Brook WS2, as the debris was left at the site. For Hubbard Brook WS5 and HJ
7 Andrews WS1 the interception capacity was assumed to decrease after deforestation, as here
8 the debris was respectively burned and removed. Furthermore, in the absence of more detailed
9 information, it was assumed that the interception capacities changed linearly during
10 deforestation towards $I_{max,change}$ and linearly recovered to I_{max} over the period T_r as well. See
11 Table 2 for the applied parameter ranges.

12 Hereafter, the long term mean transpiration can be estimated with the remaining components
13 of the long term water balance, assuming no additional gains/losses, storage changes and/or
14 data errors:

$$15 \quad \bar{E}_t = \bar{P}_e - \bar{Q}, \quad (5)$$

16 where \bar{E}_t [L T⁻¹] is the long-term mean actual transpiration,
17 \bar{P}_e [L T⁻¹] is the long-term mean effective precipitation and
18 \bar{Q} [L T⁻¹] is the long-term mean catchment runoff. Taking into account seasonality, the actual
19 mean transpiration is scaled with the ratio of long-term mean daily potential evaporation E_p
20 over the mean annual potential evaporation E_p :

21

$$22 \quad E_t(t) = \frac{E_p(t)}{E_p} * \bar{E}_t \quad (6)$$

23 Based on this, the cumulative deficit between actual transpiration and precipitation over time
24 can be estimated by means of an ‘infinite-reservoir’. In other words, the cumulative sum of

1 daily water deficits, i.e. evaporation minus precipitation, is calculated between T_0 , which is
2 the time the deficit equals zero, and T_1 , which is the time the total deficit returned to zero. The
3 maximum deficit of this period then represents the volume of water that needs to be stored to
4 provide vegetation continuous access to water throughout that time:

5
$$S_R = \max \int_{T_0}^{T_1} (E_t - P_s) dt, \quad (7)$$

6 where S_R [L] is the maximum root zone storage capacity over the time period between T_0 and
7 T_1 . See also Figure 1 for a graphical example of the calculation for the Hubbard Brook
8 catchment for one specific realization of the parameter sampling. The $S_{R,20\text{yr}}$ for drought
9 return periods of 20 years was estimated using the Gumbel extreme value distribution
10 (Gumbel, 1941) as previous work suggested that vegetation designs S_R to satisfy deficits
11 caused by dry periods with return periods of approximately 10-20 years (Gao et al., 2014; de
12 Boer-Euser et al., 2016). Thus, the maximum values of S_R for each year, as obtained by
13 equation 7, were fitted to the extreme value distribution of Gumbel, and subsequently, the
14 $S_{R,20\text{yr}}$ was determined.

15 For the study catchments that experienced logging and subsequent reforestation, it was
16 assumed that the root system converges towards a dynamic equilibrium approximately 10
17 years after reforestation. Thus, the equilibrium $S_{R,20\text{yr}}$ was estimated using only data over a
18 period that started at least 10 years after the treatment. For the growing root systems during
19 the years after reforesting, the storage capacity does not yet reach its dynamic equilibrium
20 $S_{R,20\text{yr}}$. Instead of determining an equilibrium value, the maximum occurring deficit for each
21 year was in that case considered as the maximum demand and thus as the maximum required
22 storage $S_{R,1\text{yr}}$ for that year. To make these yearly estimates, the mean transpiration was
23 determined in a similar way as stated by Equation 2. However, the assumption of no storage
24 change may not be valid for 1-year periods. In a trade-off to limit the potential bias introduced
25 by inter-annual storage changes in the catchments, the mean transpiration was determined
26 based on the 2-year water balance, thus assuming negligible storage change over these years.

27 The deficits in the months October-April are highly affected by snowfall, as estimates of the
28 effective precipitation are estimated without accounting for snow, leading to soil moisture
29 changes that spread out over an unknown longer period due to the melt process. Therefore, to
30 avoid this influence of snow, only deficits as defined by Equation 5, in the period of May –
31 September are taken into consideration, which is also the period where deficits are

1 significantly increasing due to relatively low rainfall and high transpiration rates, thus
2 causing soil moisture depletion and drought stress for the vegetation, which in turn, shapes the
3 root zone.

4 **3.2 Model-derived root zone storage capacity $S_{u,\max}$**

5 The water balance derived equilibrium $S_{R,20\text{yr}}$ as well as the dynamically changing $S_{R,1\text{yr}}$ that
6 reflects regrowth patterns in the years after treatment were compared with estimates of the
7 calibrated parameter $S_{u,\max}$, which represents the mean catchment root zone storage capacity
8 in lumped conceptual hydrological models. Due to the lack of direct observations of the
9 changes in the root zone storage capacity, this comparison was used to investigate whether the
10 estimates of the root zone storage capacity $S_{R,1\text{yr}}$, their sensitivity to land cover change and
11 their effect on hydrological functioning, can provide plausible results. Model-based estimates
12 of root zone storage capacity may be highly influenced by model formulations and
13 parameterizations. Therefore, four different hydrological models were used to derive the
14 parameter $S_{u,\max}$ in order to obtain a set of different estimates of the catchment scale root zone
15 storage capacity. The major features of the model routines for root-zone moisture tested here
16 are briefly summarized below and detailed descriptions including the relevant equations are
17 provided as supplementary material (Section S2).

18 **3.2.1 FLEX**

19 The FLEX-based model (Fenia et al., 2008) was applied in a lumped way to the catchments.
20 The model has 9 parameters, 8 of which are free calibration parameters, sampled from
21 relatively wide, uniform prior distributions. In contrast, based on the estimation of a Master
22 Recession Curve (e.g. Fenicia et al., 2006), an informed prior distribution between narrow
23 bounds could be used for determining the slow reservoir coefficient K_s .

24 The model consists of five storage components. First, a snow routine has to be run, which is a
25 simple degree-day module, similar as used in, for example, HBV (Bergström, 1976). After the
26 snow routine, the precipitation enters the interception reservoir. Here, water evaporates at
27 potential rates or, when exceeding a threshold, directly reaches the soil moisture reservoir.
28 The soil moisture routine is modelled in a similar way as the Xinanjiang model (Zhao, 1992).
29 Briefly, it contains a distribution function that determines the fraction of the catchment where
30 the storage deficit in the root zone is satisfied and that is therefore hydrologically connected
31 to the stream and generating storm runoff. From the soil moisture reservoir, water can further

1 vertically percolate down to recharge the groundwater or leave the reservoir through
2 transpiration. Transpiration is a function of maximum root zone storage $S_{u,\max}$ and the actual
3 root zone storage, similar to the functions described by Feddes et al. (1978). Water that cannot
4 be stored in the soil moisture storage then is split into preferential percolation to the
5 groundwater and runoff generating fluxes that enter a fast reservoir, which represents fast
6 responding system components such as shallow subsurface and overland flow.

7 3.2.2 HYPE

8 The HYPE model (Lindström et al., 2010) estimates soil moisture for Hydrological Response
9 Units (HRU), which is the finest calculation unit in this catchment model. In the current set-
10 up, 15 parameters were left free for calibration. Each HRU consists of a unique combination
11 of soil and land-use classes with assigned soil depths. Water input is estimated from
12 precipitation after interception and a snow module at the catchment scale, after which the
13 water enters the three defined soil layers in each HRU. Evaporation and transpiration occurs
14 in the first two layers and fast surface runoff is produced when these layers are fully saturated
15 or when rainfall rates exceeds the maximum infiltration capacities. Water can move between
16 the layers through percolation or laterally via fast flow pathways. The groundwater table is
17 fluctuating between the soil layers with the lowest soil layer normally reflecting the base flow
18 component in the hydrograph. The water balance of each HRU is calculated independently
19 and the runoff is then aggregated in a local stream with routing before entering the main
20 stream.

21

22 3.2.3 TUW

23 The TUW model (Parajka et al., 2007) is a conceptual model with a structure similar to that of
24 HBV (Bergström, 1976) and has 15 free calibration parameters. After a snow module, based
25 on a degree-day approach, water enters a soil moisture routine. From this soil moisture
26 routine, water is partitioned into runoff generating fluxes and evaporation. Here, transpiration
27 is determined as a function of maximum root zone storage $S_{u,\max}$ and actual root zone storage
28 as well. The runoff generating fluxes percolate into two series of reservoirs. A fast responding
29 reservoir with overflow outlet represents shallow subsurface and overland flow, while the
30 slower responding reservoir represents the groundwater.

1

2 **3.2.4 HYMOD**

3 HYMOD (Boyle, 2001) is similar to the applied model structure for FLEX, but only has 8
4 parameters. Besides that, the interception module and percolation from soil moisture to the
5 groundwater are missing. Nevertheless, the model accounts similarly for the partitioning of
6 transpiration and runoff generation in a soil moisture routine. Also for this model,
7 transpiration is a function of maximum storage and actual storage in the root zone. The runoff
8 generating fluxes are eventually divided over a slow reservoir, representing groundwater, and
9 a fast reservoir, representing the fast processes.

10 **3.3 Model calibration**

11 Each model was calibrated using a Monte-Carlo strategy within consecutive two year
12 windows in order to obtain a time series of root zone moisture capacities $S_{u,\max}$. FLEX, TUW
13 and HYMOD were all run 100,000 times, whereas HYPE was run 10,000 times and 20,000
14 times for HJ Andrews WS1 and the Hubbard Brook catchments respectively, due to the
15 required runtimes. The Kling-Gupta efficiency for flows (Gupta et al., 2009) and the Kling-
16 Gupta efficiency for the logarithm of the flows were simultaneously used as objective
17 functions in a multi-objective calibration approach to evaluate the model performance for
18 each window. These were selected in order to obtain rather balanced solutions that enable a
19 sufficient representation of peak flows, low flows and the water balance. The unweighted
20 Euclidian Distance D_E of the three objective functions served as an informal measure to
21 obtain these balanced solutions (e.g. Hrachowitz et al., 2014; Schoups et al., 2005):

22

23

24
$$L(\theta) = 1 - \sqrt{(1 - E_{KG})^2 + (1 - E_{\log KG})^2} \quad (8)$$

25

26 where $L(\theta)$ is the conditional probability for parameter set θ [-], E_{KG} the Kling-Gupta
27 efficiency [-], $E_{\log KG}$ the Kling-Gupta efficiency for the log of the flows [-], and E_{VE} the
28 volume error [-].

1 Eventually, a weighing method based on the GLUE-approach of Freer et al. (1996) was
 2 applied. To estimate posterior parameter distributions all solutions with Euclidian Distances
 3 smaller than 1 were maintained as feasible. The posterior distributions were then determined
 4 with the Bayes rule (cf. Freer et al., 1996):

$$5 \quad L_2(\theta) = L(\theta)^n * L_0(\theta) / C \quad (9)$$

6 where $L_0(\theta)$ is the prior parameter distribution [-], $L_2(\theta)$ is the posterior conditional
 7 probability [-], n is a weighing factor (set to 5) [-], and C a normalizing constant [-]. 5/95th
 8 model uncertainty intervals were then constructed based on the posterior conditional
 9 probabilities.

10 3.4 Trend analysis

11 To test if $S_{R,1yr}$ significantly changes following de- and subsequent reforestation, which would
 12 also indicate shifts in distinct hydrological regimes, a trend analysis, as suggested by Allen et
 13 al. (1998), was applied to the $S_{R,1yr}$ values obtained from the water balance-based method. As
 14 the sampling of interception capacities (Eq. 4) leads to $S_{R,1yr}$ values for each point in time,
 15 which are all equally likely in absence of any further knowledge, the mean of this range was
 16 assumed as an approximation of the time-dynamic character of $S_{R,1yr}$.

17 Briefly, a linear regression between the full series of the cumulative sums of $S_{R,1yr}$ in the
 18 deforested catchment and the unaffected control catchment is established and the residuals
 19 and the cumulative residuals are plotted in time. A 95%-confidence ellipse is then constructed
 20 from the residuals:

$$21 \quad X = \frac{n}{2} \cos(\alpha) \quad (10)$$

$$22 \quad Y = \frac{n}{\sqrt{n-1}} Z_{p95} \sigma_r \sin(\alpha) \quad (11)$$

23 where X presents the x-coordinates of the ellipse [T], Y represents the y-coordinates of the
 24 ellipse [L], n is the length of the time series [T], α is the angle defining the ellipse (0 - 2π)
 25 between the diagonal of the ellipse and the x-axis [-], Z_{p95} is the value belonging to a
 26 probability of 95% of the standard student t-distribution [-] and σ_r is the standard deviation of
 27 the residuals (assuming a normal distribution) [L].

1 When the cumulative sums of the residuals plot outside the 95%-confidence interval defined
2 by the ellipse, the null-hypothesis that the time series are homogeneous is rejected. In that
3 case, the residuals from this linear regression where residual values change from either solely
4 increasing to decreasing or vice versa, can then be used to identify different sub-periods in
5 time.

6 Thus, in a second step, for each identified sub-period a new regression, with new (cumulative)
7 residuals, can be used to check homogeneity for these sub-periods. In a similar way as before,
8 when the cumulative residuals of these sub-periods now plot within the accompanying newly
9 created 95%-confidence ellipse, the two series are homogeneous for these sub-periods. In
10 other words, the two time series show a consistent behavior over this particular period.

11

12 **3.5 Model with time-dynamic formulation of $S_{u,\max}$**

13 In a last step, the FLEX model was reformulated to allow for a time-dynamic representation
14 of the parameter $S_{u,\max}$, reflecting the root zone storage capacity.

15 As a reference, the long-term water balance derived root zone storage capacity $S_{R,20\text{yr}}$ was
16 used as a static formulation of $S_{u,\max}$ in the model, and thus kept constant in time. The
17 remaining parameters were calibrated using the calibration strategy outlined above over a
18 period starting with the treatment in the individual catchments until at least 15 years after the
19 end of the treatment. This was done to focus on the period under change (i.e. vegetation
20 removal and recovery), during which the differences between static and dynamic formulations
21 of $S_{u,\max}$ are assumed to be most pronounced.

22 To test the effect of a dynamic formulation of $S_{u,\max}$ as a function of forest regrowth, the
23 calibration was run with a temporally evolving series of root zone storage capacity. The time-
24 dynamic series of $S_{u,\max}$ were obtained from a relatively simple growth function, the Weibull
25 function (Weibull, 1951):

26

27

28 $S_{u,\max}(t) = S_{R,20\text{yr}} \left(1 - e^{-a t^b}\right), \quad (11)$

1 where $S_{u,\max}(t)$ is the root zone storage capacity t time steps after reforestation [L], $S_{R,20\text{yr}}$ is
2 the equilibrium value [L], and a [T^{-1}] and b [-] are shape parameters. In the absence of more
3 information, this equation was selected as a first, simple way of incorporating the time-
4 dynamic character of the root zone storage capacity in a conceptual hydrological model. In
5 this way, root growth is exclusively determined dependent on time, whereas the shape-
6 parameters a and b merely implicitly reflect the influence of other factors, such as climatic
7 forcing in a lumped way. These parameters were estimated based on qualitative judgement so
8 that $S_{u,\max}(t)$ coincides well with the suite of $S_{R1\text{yr}}$ values after logging. In other words, the
9 values were chosen by trial and error in such a way, that the time-dynamic formulation of
10 $S_{u,\max}(t)$ shows a visually good correspondence with the $S_{R1\text{yr}}$ values. This approach was
11 followed to filter out the short term fluctuations in the $S_{R1\text{yr}}$ values, which is not warranted by
12 this equation. Note that this rather simple approach is merely meant as a proof-of-concept for
13 a dynamic formulation of $S_{u,\max}$.

14 In addition, the remaining parameter directly related to vegetation, the interception capacity
15 (I_{\max}), was also assigned a time-dynamic formulation. Here, the same growth function was
16 applied (Eq. 11), but the shape of the growth function was assumed fixed (i.e. growth
17 parameters a and b were fixed to values of 0.001 [day^{-1}] and 1 [-]) loosely based on the
18 posterior ranges of the window calibrations, with qualitative judgement as well. This growth
19 function was used to ensure the degrees of freedom for both the time-variant and the time-
20 invariant models, leaving the equilibrium value of the interception capacity as the only free
21 calibration parameter for this process. Note that the empirically parameterized growth
22 functions can be readily extended and/or replaced by more mechanistic, process-based
23 descriptions of vegetation growth if warranted by the available data and was here merely used
24 to test the effect of considering changes in vegetation on the skill of models to reproduce
25 hydrological response dynamics.

26 To assess the performance of the dynamic model compared to the time-invariant formulation,
27 beyond the calibration objective functions, model skill in reproducing 28 hydrological
28 signatures was evaluated (Sivapalan et al., 2003). Even though the signatures are not always
29 fully independent of each other, this larger set of measures allows a more complete evaluation
30 of the model skill as, ideally, the model should be able to simultaneously reproduce all
31 signatures. An overview of the signatures is given in Table 3. The results of the comparison

1 were quantified on the basis of the probability of improvement for each signature (Nijzink et
2 al., 2016):

3 $P_{I,S} = P(S_{dyn} > S_{stat}) = \sum_{i=1}^n P(S_{dyn} > S_{stat} | S_{dyn} = r_i)P(S_{dyn} = r_i)$ (12)

4 where S_{dyn} and S_{stat} are the distributions of the signature performance metrics of the dynamic
5 and static model, respectively, for the set of all feasible solutions retained from calibration, r_i
6 is a single realization from the distribution of S_{dyn} and n is the total number of realizations of
7 the S_{dyn} distribution. For $P_{I,S} > 0.5$ it is then more likely that the dynamic model outperforms
8 the static model with respect to the signature under consideration, and vice versa for $P_{I,S} < 0.5$.
9 The signature performance metrics that were used are the relative error for single-valued
10 signatures and the Nash-Sutcliffe efficiency (Nash and Sutcliffe, 1970) for signatures that
11 represent a time series.

12 In addition, as a more quantitative measure, the Ranked Probability Score, giving information
13 on the magnitude of model improvement or deterioration, was calculated (Wilks, 2005):

14 $S_{RP} = \frac{1}{M-1} \sum_{m=1}^M \left[\left(\sum_{k=1}^m p_k \right) - \left(\sum_{k=1}^m o_k \right) \right]^2$ (13)

15 where M is the number of feasible solutions, p_k the probability of a certain signature
16 performance to occur and o_k the probability of the observation to occur (either 1 or 0, as there
17 is only a single observation). Briefly, the S_{RP} represents the area enclosed between the
18 cumulative probability distribution obtained by model results and the cumulative probability
19 distribution of the observations. Thus, when modelled and observed cumulative probabilities
20 are identical, the enclosed area goes to zero. Therefore, the difference between the S_{RP} for the
21 feasible set of solutions for the time-variant and time-invariant model formulation was used in
22 the comparison, identifying which model is quantitatively closer to the observation.

23

24 **4 Results**

25 **4.1 Deforestation and changes in hydrological response dynamics**

26 We found that the three deforested catchments in the two research forests show on balance
27 similar response dynamics after the logging of the catchments (Fig.2). This supports the

1 findings from previous studies of these catchments (Andréassian, 2004; Bosch and Hewlett,
2 1982; Hornbeck et al., 1997; Rothacher et al., 1967). More specifically, it was found that the
3 observed annual runoff coefficients for HJ Andrews WS1 and Hubbard Brook WS2 (Fig.
4 2a,b) change after logging of the catchments, also in comparison with the adjacent,
5 undisturbed reference watersheds. Right after deforestation, runoff coefficients increase,
6 which is followed by a gradual decrease.

7 The annual autocorrelation coefficients with a 1-day lag time are generally lower after logging
8 than in the years before the change, which can be seen in particular from Figures 2e and 2f as
9 here a long pre-treatment time series record is available. Nevertheless, the climatic influence
10 cannot be ignored here, as the reference watershed shows a similar pattern. Only for Hubbard
11 Brook WS5 (Fig. 2f), the autocorrelation shows reduced values in the first years after logging.
12 Thus, the flows at any time $t+1$ are less dependent on the flows at t , which points towards less
13 memory and thus less storage in the system (i.e. reduced S_R), leading to increased peak flows,
14 similar to the reports of, for example, Patric and Reinhart (1971) for one of the Fernow
15 experiments.

16 The declining limb density for HJ Andrews WS1 (Fig. 2g) shows increased values right after
17 deforestation, whereas longer after deforestation the values seem to plot closer to the values
18 obtained from the reference watershed. This indicates that for the same number of peaks less
19 time was needed for the recession in the hydrograph in the early years after logging. In
20 contrast, the rising limb density shows increased values during and right after deforestation
21 for Hubbard Brook WS2 and WS5 (Fig 2k-2l), compared to the reference watershed. Here,
22 less time was needed for the rising part of the hydrograph in the more early years after
23 logging. Thus, the recession seems to be affected in HJ Andrews WS1, whereas the Hubbard
24 Brook watersheds exhibits a quicker rise of the hydrograph.

25 Eventually, the flow duration curves, as shown in Figures 2m-2o, indicate a higher variability
26 of flows, as the years following deforestation plot with an increased steepness of the flow
27 duration curve, i.e. a higher flashiness. This increased flashiness of the catchments after
28 deforestation can also be noted from the hydrographs shown in Figure 3. The peaks in the
29 hydrographs are generally higher, and the flows return faster to the baseflow values in the
30 years right after deforestation than some years 1 later after some forest regrowth, all with
31 similar values for the yearly sums of precipitation and potential evaporation.

1 **4.2 Temporal evolution of S_R and $S_{u,max}$**

2 The observed changes in the hydrological response of the study catchments (as discussed
3 above) were also clearly reflected in the temporal evolution of the root zone storage capacities
4 as described by the catchment models (Fig. 4). The models all exhibited Kling-Gupta
5 efficiencies ranging between 0.5 and 0.8 and Kling-Gupta efficiencies of the log of the flows
6 between 0.2 and 0.8 (see the supplementary material Figures S5-7, with all posterior
7 parameter distributions in Figures S10-S27, and the number of feasible solutions in Tables
8 S5-S7). Comparing the water balance and model-derived estimates of root zone storage
9 capacity S_R and $S_{u,max}$, respectively, then showed that they exhibit very similar patterns in the
10 study catchments. Especially for HJ Andrews WS1 and Hubbard Brook WS2, root zone
11 storage capacities sharply decreased after deforestation and gradually recovered during
12 regrowth towards a dynamic equilibrium of climate and vegetation, whereas the undisturbed
13 reference catchments of HJ Andrews WS2 and Hubbard Brook WS3 showed a rather constant
14 signal over the full period (see the supplementary material Figure S8).

15 The HJ Andrews WS1 shows the clearest signal when looking at the water balance derived
16 S_R , as can be seen by the green shaded area in Figure 4a. Before deforestation, the root zone
17 storage capacity $S_{R,1yr}$ was found to be around 400mm. During deforestation, the $S_{R,1yr}$
18 required to provide the remaining vegetation with sufficient and continuous access to water
19 decreased from around 400 mm to 200 mm. For the first 4-6 years after deforestation the
20 $S_{R,1yr}$ increased again, reflecting the increased water demand of vegetation with the regrowth
21 of the forest. In addition, it was observed that in the period 1971- 1978 $S_{R,1yr}$ slowly decreased
22 again in HJ Andrews.

23 The four models show a similar pronounced decrease of the calibrated, feasible set of $S_{u,max}$
24 during deforestation and a subsequent gradual increase over the first years after deforestation.
25 The model concepts, thus our assumptions about nature, can therefore only account for the
26 changes in hydrological response dynamics of a catchment, when calibrated in a window
27 calibration approach with different parameterizations for each time frame. The absolute
28 values of $S_{u,max}$ obtained from the most parsimonious HYMOD and FLEX models (both 8
29 free calibration parameters) show a somewhat higher similarity to $S_{R,1yr}$ and its temporal
30 evolution than the values from the other two models. In spite of similar general patterns in
31 $S_{u,max}$, the higher number of parameters in TUW (i.e. 15) result, due to compensation effects
32 between individual parameters, in wider uncertainty bounds which are less sensitive to

1 change. It was also observed that in particular TUW overestimates $S_{u,\max}$ compared to $S_{R,1yr}$,
2 which can be attributed to the absence of an interception reservoir, leading to a root zone that
3 has to satisfy not only transpiration but all evaporative fluxes.

4 Hubbard Brook WS2 exhibits a similarly clear decrease in root zone storage capacity as a
5 response to deforestation, as shown in Figure 4b. The water balance-based $S_{R,1yr}$ estimates
6 approach values of zero during and right after deforestation. In these years the catchment was
7 treated with herbicides, removing effectively any vegetation, thereby minimizing
8 transpiration. In this catchment a more gradual regrowth pattern occurred, which continued
9 after logging started in 1966 until around 1983.

10 Generally, the models applied in Hubbard Brook WS2 show similar behavior as in the HJ
11 Andrews catchment. The calibrated $S_{u,\max}$ clearly follows the temporal pattern of $S_{R,1yr}$,
12 reflecting the pronounced effects of de- and reforestation. It can, however, also be observed
13 that the absolute values of $S_{u,\max}$ exceed the $S_{R,1yr}$ estimates. While FLEX on balance exhibits
14 the closest resemblance between the two values, in particular the TUW model exhibits wide
15 uncertainty bounds with elevated $S_{u,\max}$ values. Besides the role of interception evaporation,
16 which is only explicitly accounted for in FLEX, the results are also linked to the fact that the
17 humid climatic conditions with little seasonality reduces the importance of the model
18 parameter $S_{u,\max}$, and makes it thereby more difficult to identify by calibration. The parameter
19 is most important for lengthy dry periods when vegetation needs enough storage to ensure
20 continuous access to water.

21 The temporal variation in S_R in Hubbard Brook WS5 does not show such a distinct signal as
22 in the other two study catchments (Figure 4c). Moreover, it can be noted that in the summers
23 of 1984 and 1985 the values of $S_{R,1yr}$ are relatively high. Nevertheless, the model based
24 values of $S_{u,\max}$ show again similar dynamics as the water balance based $S_{R,1yr}$ values. TUW
25 and HYMOD show again higher model based values, but also FLEX is now overestimating
26 the root zone storage capacity.

27 **4.3 Process understanding - trend analysis and change in hydrological 28 regimes**

29 The trend analysis for water-balance derived values of $S_{R,1yr}$ suggests that for all three study
30 catchments significantly different hydrological regimes in time can be identified before and
31 after deforestation, linked to changes in $S_{R,1yr}$ (Fig. 7). For all three catchments, the

1 cumulative residuals plot outside the 95%-confidence ellipse, indicating that the time series
2 obtained in the control catchments and the deforested catchments are not homogeneous
3 (Figures 7g-7i).

4 Rather obvious break points can be identified in the residuals plots for the catchments HJ
5 Andrews WS1 and Hubbard Brook WS2 (Fig. 7d-7e). Splitting up the $S_{R,1yr}$ time series
6 according to these break points into the periods before deforestation, deforestation and
7 recovery resulted in three individually homogenous time series that are significantly different
8 from each other, indicating switches in the hydrological regimes. The results shown in Figure
9 4 indicate that these catchments developed a rather stable root zone storage capacity sometime
10 after the start of deforestation (for HJ Andrews WS1 after 1964, for Hubbard Brook WS2
11 after 1967). Hence, recovery and deforestation balanced each other, leading to a temporary
12 equilibrium. The recovery signal then becomes more dominant in the years after
13 deforestation. The third homogenous period suggests that the root zone storage capacity
14 reached a dynamic equilibrium without any further systematic changes. This can be
15 interpreted in the way that in the HJ Andrews WS1 hydrological recovery after deforestation
16 due to the recovery of the root zone store capacity took about 6-9 years (Fig. 7p), while
17 Hubbard Brook WS2 required 10-13 years for hydrological recovery (Fig. 7q). This strongly
18 supports the results of Hornbeck et al. (2014), who reported changes in water yield for WS2
19 for up to year 12 after deforestation.

20 The identification of different periods is less obvious for Hubbard Brook WS5, but the two
21 time series of control catchment and treated catchment are significantly different (see the
22 cumulative residuals in Figure 7i). Nevertheless, the most obvious break point in residuals can
23 be found in 1989 (Figure 7f). In addition, it can be noted that turning points also exist in 1983
24 and 1985. These years can be used to split the time series into four groups (leading to the
25 periods of 1964-1982, 1983-1985, 1986-1989 and 1990-2009 for further analysis). The
26 cumulative residuals from the new regressions, based on the grouping, plot within the
27 confidence bounds again, and show a period with deforestation (1983-1985) and recovery
28 (1986-1989). Mou et al. (1993) reported similar findings with the highest biomass
29 accumulation in 1986 and 1988, and slower vegetation growth in the early years. Therefore,
30 full recovery took 5-6 years in Hubbard Brook WS5.

1 4.4 Time-variant model formulation

2 The adjusted model routine for FLEX, which uses a dynamic time series of $S_{u,\max}$, generated
3 with the Weibull growth function (Eq.11), resulted in a rather small impact on the overall
4 model performance in terms of the calibration objective function values (Figure 8b, 8d, 8f)
5 compared to the time-invariant formulation of the model. The strongest improvements for
6 calibration were observed for the dynamic formulation of FLEX for HJ Andrews WS1 and
7 Hubbard Brook WS2 (Figures 8b and 8d), which reflects the rather clear signal from
8 deforestation in these catchments.

9 Evaluating a set of hydrological signatures suggests that the dynamic formulation of $S_{u,\max}$
10 allows the model to have a higher probability to better reproduce most of the signatures tested
11 here (51% of all signatures in the three catchments) as shown in Figure 9a. A similar pattern
12 is obtained for the more quantitative S_{RP} (Figure 9b), where in 52% of the cases improvements
13 are observed. Most signatures for HJ Andrews WS1 show a high probability of improvement,
14 with a maximum $P_{I,S} = 0.69$ (for $S_{Q95,winter}$) and an average $P_{I,S} = 0.55$. Considering the large
15 difference between the deforested situation and the new equilibrium situation of about 200
16 mm, this supports the hypothesis that here a time-variant formulation of $S_{u,\max}$ does provide
17 means for an improved process representation and, thus, hydrological signatures. Here,
18 improvements are observed especially in the high flows in summer ($S_{Q5,summer}$, $S_{Q50,summer}$) and
19 peak flows (e.g. S_{Peaks} , $S_{Peaks,summer}$, $S_{Peaks,winter}$), that illustrates that the root zone storage
20 affects mostly the fast responding components of the system.

21 At Hubbard Brook WS2 a more variable pattern is shown in the ability of the model to
22 reproduce the hydrological signatures. It is interesting to note that the low flows (S_{Q95} ,
23 $S_{Q95,summer}$, $S_{Q50,summer}$) improve, opposed to the expectation raised by the argumentation for
24 HJ Andrews WS1 that peak flows and high flows should improve. In this case, the peaks are
25 too high for the time-dynamic model.

26 The probabilities of improvement for the signatures in Hubbard Brook WS5 show an even
27 less clear signal, the model cannot clearly identify a preference for either a dynamic or static
28 formulation of $S_{u,\max}$ (relatively white colors in Fig. 9). This absence of a clear preference can
29 be related to the observed patterns in water balance derived S_R (Figure 4c), which does not
30 show a very clear signal after deforestation as well, indicating that the root zone storage
31 capacity is of less importance in this humid region characterized by limited seasonality.

1 **5 Discussion**

2 **5.1 Deforestation and changes in hydrological response dynamics**

3 The changes found in the runoff behavior of the deforested catchments point towards shifts in
4 the yearly sums of transpiration, which can, except for climatic variation, be linked to the
5 regrowth of vegetation that takes place at a similar pace as the changes in hydrological
6 dynamics. This coincidence of regrowth dynamics and evolution of runoff coefficients was
7 not only noticed by Hornbeck et al. (2014) for the Hubbard Brook, but was also previously
8 acknowledged for example by Swift and Swank (1981) in the Coweeta experiment or Kuczera
9 (1987) for eucalypt regrowth after forest fires.

10 Therefore, the key role of vegetation in this partitioning between runoff and transpiration
11 (Donohue et al., 2012), or more specifically root zones (Gentine et al., 2012), necessarily
12 leads to a change in runoff coefficients when vegetation is removed. Similarly, Gao et al.
13 (2014) found a strong correlation between root zone storage capacities and runoff coefficients
14 in more than 300 US catchments, which lends further support to the hypothesis that root zone
15 storage capacities may have decreased in deforested catchments right after removal of the
16 vegetation.

17 **5.2 Temporal evolution of S_R and $S_{u,\max}$**

18 The differences between the Hubbard Brook catchments and HJ Andrews catchments can be
19 related to climatic conditions. In spite of the high annual precipitation volumes, high $S_{R,1yr}$
20 values are plausible for HJ Andrews WS1 given the marked seasonality of the precipitation in
21 the Mediterranean climate (Koeppen-Geiger class Csb) and the approximately 6 months phase
22 shift between precipitation and potential evaporation peaks in the study catchment, which
23 dictates that the storage capacities need to be large enough to store precipitation falling mostly
24 during winter throughout the extended dry periods with higher energy supply throughout the
25 rest of the year (Gao et al., 2014). At the same time, low $S_{R,1yr}$ values in Hubbard Brook WS2
26 can be related to the relatively humid climate and the absence of pronounced rainfall
27 seasonality strongly reduces storage requirements.

28 It can also be argued that there is a strong influence of the inter-annual climatic variability on
29 the estimated root zone storage capacities. For example, the marked increase in $S_{R,1yr}$ in
30 Hubbard Brook WS2 in 1985 rather points towards an exceptional year, in terms of

1 climatological factors, than a sudden expansion of the root zone. It can also be observed from
2 Figure 3a that the runoff coefficient was relatively low for 1985, suggesting either increased
3 evaporation or a storage change. A combination of a relatively long period of low rainfall
4 amounts and high potential evaporation, as can be noted by the relatively high mean annual
5 potential evaporation on top of Figure 4b, may have led to a high demand in 1985. Parts of the
6 vegetation may not have survived these high-demand conditions due to insufficient access to
7 water, explaining the dip in $S_{R,1yr}$ for the following year, which is also in agreement with
8 reduced growth rates of trees after droughts as observed by for example Bréda et al. (2006).
9 The hydrographs of 1984-1985 (Figure 6a) and 1986-1987 (Figure 6b) also show that July-
10 August 1985 was exceptionally dry, whereas the next year in August 1986 the catchment
11 seems to have increased peak flows. This either points towards an actual low storage capacity
12 due to contraction of the roots during the dry summer or a low need of the system to use the
13 existing capacity, for instance to recover other vital aspects of the system.

14 Nevertheless, Hubbard Brook WS2 does not show a clear signal of reduced root zone storage,
15 followed by a gradual regrowth. Here, the forest was removed in a whole-tree harvest in
16 winter '83-'84 followed by natural regrowth. The summers of 1984 and 1985 were very dry
17 summers, as also reflected by the high values of $S_{R,1yr}$. The young system had already
18 developed enough roots before these dry periods to have access to a sufficiently large water
19 volume to survive this summer. This is plausible, as the period of the highest deficit occurred
20 in mid-July and lasted until approximately the end of September, thus long after the beginning
21 of the growing season, allowing enough time for an initial growth and development of young
22 roots from April until mid-July. In addition, the composition of the new forest differed from
23 the old forest with more pin cherry (*Prunus pensylvanica*) and paper birch (*Betula*
24 *papyrifera*). This supports the statements of a quick regeneration as these species have a high
25 growth rate and reach canopy closure in a few years. Furthermore, the forest was not treated
26 with either herbicides (Hubbard Brook WS2) or burned (HJ Andrews WS1), leaving enough
27 low shrubs and herbs to maintain some level of transpiration (Hughes and Fahey, 1991;
28 Martin, 1988). It can thus be argued, similar to Li et al. (2007), that the remaining vegetation
29 experienced less competition and could increase root water uptake efficiency and transpiration
30 per unit leaf area. This is in agreement with Hughes and Fahey (1991), who also stated that
31 several species benefited from the removal of canopies and newly available resources in this
32 catchment. Lastly, several other authors related the absence of a clear change in hydrological
33 dynamics to the severe soil disturbance in this catchment (Hornbeck et al., 1997; Johnson et

1 al., 1991). These disturbances lead to extra compaction, whereas at the same time species
2 were changing, effectively masking any changes in runoff dynamics.

3 **5.3 Process understanding - trend analysis and change in hydrological
4 regimes**

5 The found recovery periods correspond to recovery time scales for forest systems as reported
6 elsewhere (e.g. Brown et al., 2005; Hornbeck et al., 2014; Elliott et al., 2016), who found that
7 catchments reach a new equilibrium with a similar timescale as reported here with the direct
8 link to the parameter describing the catchment-scale root zone storage capacity. The
9 timescales are also in agreement with regression models to predict water yield after logging of
10 Douglass (1983), who assumed a duration of water yield increases of 12 years for coniferous
11 catchments.

12 The timescales found here are around 10 years (here 5-13 years for the catchments under
13 consideration), but will probably depend on climatic factors and vegetation type. HJ Andrews
14 WS1 has a recovery (6-9 years) slightly shorter compared to Hubbard Brook WS2 (10-13
15 years), which could depend on the different climatological conditions of the catchments.
16 Nevertheless, it could also be argued that especially the spraying of herbicides had a strong
17 impact on the recovery of vegetation in Hubbard Brook WS2, as the Hubbard Brook WS5
18 does not show such a distinct recovery signal.

19 **5.4 Time-variant model formulation**

20 It was found that a time dynamic formulation of $S_{u,\max}$ merely improved the high and peak
21 flow signatures for HJ Andrews WS1. Other authors also suggested previously (e.g. de Boer-
22 Euser et al., 2016; Euser et al., 2015; Oudin et al., 2004) that that the root zone storage affects
23 mostly the fast responding components of the system, by providing a buffer to storm
24 response. Fulfilling its function as a storage reservoir for plant available water, modelled
25 transpiration is significantly reduced post-deforestation, which in turn results in increased
26 runoff coefficients (cf. Gao et al., 2014), which have been frequently reported for post-
27 deforestation periods by earlier studies (e.g. Hornbeck et al., 2014; Rothacher, 1970; Swift
28 and Swank, 1981)

29 Nevertheless, signatures considering the peak flows did not improve for the Hubbard Brook
30 catchments. Apparently, the model with a constant, and thus higher, $S_{u,\max}$ stored water in the

1 root zone, reducing recharge to the groundwater reservoir that maintains the lower flows and
2 buffering more water, reducing the peaks. This can also be clearly seen from the hydrographs
3 (Figure 10), where the later part of the recession in the late-summer months is much better
4 captured by the time-dynamic model. Nevertheless, the peaks are too high for the time-
5 dynamic model, which here is linked to an insufficient representation of snow-related
6 processes, as can be seen from the hydrograph (April-May) as well, and possibly by an
7 inadequate interception growth function, both leading to too high amounts of effective
8 precipitation entering the root zone. An adjustment of these processes would have resulted in
9 less infiltration and a smaller root zone storage capacity.

10 It was acknowledged previously by several authors that certain model parameters may need
11 time-dynamic formulations, like Waichler et al. (2005) with time-dynamic formulations of
12 leaf area index and overstore height for the DHSVM model. In addition, Westra et al. (2014)
13 captured long term dynamics in the storage parameter of the GR4J model with a trend
14 correction, in fact leading to a similar model behavior as with the Weibull growth function in
15 this study. Nevertheless, they only hypothesized about the actual hydrological reasons for
16 this, which aimed at the changing number of farmer dams in the catchment. The results
17 presented here indicate that vegetation, and especially root zone dynamics, has a strong
18 impact on the long term non-stationarity of model parameters. The simple Weibull equation
19 can be used as an extra equation in conceptual hydrological models to more closely reflect the
20 dynamics of vegetation. The additional growth parameters may be left for calibration, but can
21 also be estimated from simple water balance-based estimations of the root zone storage. In
22 this way, the extra parameters should not add any uncertainty to the model outcomes.

23

24 **5.5 General Limitations**

25 The results presented here depend on the quality of the data and several assumptions made in
26 the calculations. A limiting factor is that the potential evaporation is determined from
27 temperature only, leading to values that may be relatively low and water balances that may
28 not close completely. Generally, this would lead to a discrepancy between the modelled
29 $S_{u,\max}$, where potential evaporation is directly used, and the water balance-estimates of S_R .
30 The models will probably generate higher root zone storages in order to compensate for the

1 rather low potential evaporation. This can also be noted when looking at Figure 4 for several
2 models.

3 In addition, the assumption that the water balance closes in the 2-year periods under
4 consideration may in reality be often violated. It can be argued that the estimated transpiration
5 for the calculation of S_R represents an upper boundary, when storage changes are ignored.
6 This would lead to estimates of S_R that may be lower than presented here. Nevertheless,
7 attempts with 5-year water balances to reduce the influence of storage changes (see the
8 Supplementary Material Figure S9), showed that similar patterns were obtained. Values here
9 were slightly lower due to more averaging in the estimation of the transpiration by the longer
10 time period used for the water balance. Nevertheless, still a strong decrease after deforestation
11 and gradual recovery can be observed.

12 The raised issues here can be fully avoided when, instead of a water balance-based estimation
13 of the transpiration, remote sensing products are used to estimate the transpiration, similar to
14 Wang-Erlandsson et al. (2016). However, water balance-based estimates may provide a rather
15 quick solution.

16 The transpiration estimates were also only corrected for interception evaporation, thus
17 assuming a negligible amount of soil evaporation. Making this additional separation is
18 typically not warranted by the available data and would result in additional uncertainty. The
19 transpiration estimates presented here merely represent an upper limit of transpiration and will
20 be lower in reality due to soil evaporation. Thus, the values for $S_{R,1yr}$ may be expected to be
21 lower in reality as well.

22

23 **6 Conclusion**

24 In this study, three deforested catchments (HJ Andrews WS1, Hubbard Brook WS2 and WS5)
25 were investigated to assess the dynamic character of root zone storage capacities using water
26 balance, trend analysis, four different hydrological models and one modified model version.
27 Root zone storage capacities were estimated based on a simple water balance approach.
28 Results demonstrate a good correspondence between water-balance derived root zone storage
29 capacities and values obtained by a 2-year moving window calibration of four distinct
30 hydrological models.

1 There are significant changes in root zone storage capacity after deforestation, which were
2 detected by both, a water-balance based method and the calibration of hydrological models in
3 two of the three catchments. More specifically, root zone storage capacities showed for HJ
4 Andrews WS1 and Hubbard Brook WS2 a sharp decrease in root zone storage capacities
5 immediately after deforestation with a gradual recovery towards a new equilibrium. This
6 could to a large extent explain post-treatment changes to the hydrological regime. These
7 signals were however not clearly observed for Hubbard Brook WS5, probably due to soil
8 disturbance, a new vegetation composition and a climatologically exceptional year.
9 Nevertheless, trend analysis showed significant differences for all three catchments with their
10 corresponding, undisturbed reference watersheds. Based on this, recovery times were
11 estimated to be between 5-13 years for the three catchments under consideration.

12 These findings underline the fact that root zone storage capacities in hydrological models,
13 which are more often than not treated as constant in time, may need time-dynamic
14 formulations with reductions after logging and gradual regrowth afterwards. Therefore, one of
15 the models was subsequently formulated with a time-dynamic description of root zone storage
16 capacity. Particularly under climatic conditions with pronounced seasonality and phase shifts
17 between precipitation and evaporation, this resulted in improvements in model performance
18 as evaluated by 28 hydrological signatures.

19 Even though this more complex system behavior may lead to extra unknown growth
20 parameters, it has been shown here that a simple equation, reflecting the long-term growth of
21 the system, can already suffice for a time-dynamic estimation of this crucial hydrological
22 parameter. Therefore, this study clearly shows that observed changes in runoff characteristics
23 after land cover changes can be linked to relatively simple time-dynamic formulations of
24 vegetation related model parameters.

25

26 **Acknowledgements**

27 We would like to acknowledge the European Commission FP7 funded research project
28 “Sharing Water-related Information to Tackle Changes in the Hydrosphere– for Operational
29 Needs” (SWITCH-ON, grant agreement number 603587), as this study was conducted within
30 the context of SWITCH-ON as an example of scientific potential when using open data for
31 collaborative research in hydrology.

1 Open Data were provided by the the Hubbard Brook Ecosystem Study (HBES), which is a
2 collaborative effort at the Hubbard Brook Experimental Forest which is operated and
3 maintained by the USDA Forest Service Northern Research Station, Newtown Square, PA,
4 USA.

5 Open Data were provided by the HJ Andrews Experimental Forest research program, funded
6 by the National Science Foundation's Long-Term Ecological Research Program (DEB 08-
7 23380), US Forest Service Pacific Northwest Research Station, and Oregon State University.

8

1 **References**

2

3 Alila, Y., Kuraś, P. K., Schnorbus, M., and Hudson, R.: Forests and floods: A new paradigm
4 sheds light on age-old controversies, *Water Resources Research*, 45, n/a-n/a,
5 10.1029/2008WR007207, 2009.

6 Allen, C. D., Macalady, A. K., Chenchouni, H., Bachelet, D., McDowell, N., Vennetier, M.,
7 Kitzberger, T., Rigling, A., Breshears, D. D., Hogg, E. H., Gonzalez, P., Fensham, R., Zhang,
8 Z., Castro, J., Demidova, N., Lim, J.-H., Allard, G., Running, S. W., Semerci, A., and Cobb,
9 N.: A global overview of drought and heat-induced tree mortality reveals emerging climate
10 change risks for forests, *Forest Ecology and Management*, 259, 660-684,
11 <http://dx.doi.org/10.1016/j.foreco.2009.09.001>, 2010.

12 Allen, R. G., Pereira, L. S., Raes, D., and Smith, M.: Crop evapotranspiration-Guidelines for
13 computing crop water requirements-FAO Irrigation and drainage paper 56, FAO, Rome, 300,
14 D05109, 1998.

15 Allison, G. B., Cook, P. G., Barnett, S. R., Walker, G. R., Jolly, I. D., and Hughes, M. W.:
16 Land clearance and river salinisation in the western Murray Basin, Australia, *Journal of
17 Hydrology*, 119, 1-20, [http://dx.doi.org/10.1016/0022-1694\(90\)90030-2](http://dx.doi.org/10.1016/0022-1694(90)90030-2), 1990.

18 Andersson, L., and Arheimer, B.: Consequences of changed wetness on riverine nitrogen –
19 human impact on retention vs. natural climatic variability, *Regional Environmental Change*,
20 2, 93-105, 10.1007/s101130100024, 2001.

21 Andréassian, V.: Waters and forests: from historical controversy to scientific debate, *Journal
22 of Hydrology*, 291, 1-27, <http://dx.doi.org/10.1016/j.jhydrol.2003.12.015>, 2004.

23 Bathurst, J. C., Ewen, J., Parkin, G., O'Connell, P. E., and Cooper, J. D.: Validation of
24 catchment models for predicting land-use and climate change impacts. 3. Blind validation for
25 internal and outlet responses, *Journal of Hydrology*, 287, 74-94,
26 <http://dx.doi.org/10.1016/j.jhydrol.2003.09.021>, 2004.

27 Bergström, S.: Development and application of a conceptual runoff model for Scandinavian
28 catchments. SMHI Reports RHO, Norrköping, 1976.

29 Bergström, S.: The HBV model: Its structure and applications, Swedish Meteorological and
30 Hydrological Institute, 1992.

31 Black, P. E.: WATERSHED FUNCTIONS1, *JAWRA Journal of the American Water
32 Resources Association*, 33, 1-11, 10.1111/j.1752-1688.1997.tb04077.x, 1997.

33 Bosch, J. M., and Hewlett, J. D.: A review of catchment experiments to determine the effect
34 of vegetation changes on water yield and evapotranspiration, *Journal of Hydrology*, 55, 3-23,
35 [http://dx.doi.org/10.1016/0022-1694\(82\)90117-2](http://dx.doi.org/10.1016/0022-1694(82)90117-2), 1982.

36 Boyle, D. P.: Multicriteria calibration of hydrologic models, 2001.

37 Brath, A., Montanari, A., and Moretti, G.: Assessing the effect on flood frequency of land use
38 change via hydrological simulation (with uncertainty), *Journal of Hydrology*, 324, 141-153,
39 <http://dx.doi.org/10.1016/j.jhydrol.2005.10.001>, 2006.

1 Bréda, N., Huc, R., Granier, A., and Dreyer, E.: Temperate forest trees and stands under
2 severe drought: a review of ecophysiological responses, adaptation processes and long-term
3 consequences, *Ann. For. Sci.*, 63, 625-644, 2006.

4 Breuer, L., Eckhardt, K., and Frede, H.-G.: Plant parameter values for models in temperate
5 climates, *Ecological Modelling*, 169, 237-293, [http://dx.doi.org/10.1016/S0304-3800\(03\)00274-6](http://dx.doi.org/10.1016/S0304-3800(03)00274-6), 2003.

7 Brown, A. E., Zhang, L., McMahon, T. A., Western, A. W., and Vertessy, R. A.: A review of
8 paired catchment studies for determining changes in water yield resulting from alterations in
9 vegetation, *Journal of Hydrology*, 310, 28-61,
10 <http://dx.doi.org/10.1016/j.jhydrol.2004.12.010>, 2005.

11 Brunner, I., Herzog, C., Dawes, M. A., Arend, M., and Sperisen, C.: How tree roots respond
12 to drought, *Frontiers in Plant Science*, 6, 547, 10.3389/fpls.2015.00547, 2015.

13 Brunner, P., and Simmons, C. T.: HydroGeoSphere: A Fully Integrated, Physically Based
14 Hydrological Model, *Ground Water*, 50, 170-176, 10.1111/j.1745-6584.2011.00882.x, 2012.

15 Campbell, J.: Hubbard Brook Experimental Forest (USDA Forest Service): Daily Streamflow
16 by Watershed, 1956 - present, <http://www.hubbardbrook.org/data/dataset.php?id=2>, 2014a.

17 Campbell, J.: Hubbard Brook Experimental Forest (US Forest Service): Daily Precipitation
18 Standard Rain Gage Measurements, 1956 - present,
19 <http://www.hubbardbrook.org/data/dataset.php?id=13>, 2014b.

20 Campbell, J.: Hubbard Brook Experimental Forest (USDA Forest Service): Daily Maximum
21 and Minimum Temperature Records, 1955 - present,
22 <http://www.hubbardbrook.org/data/dataset.php?id=59>, 2014c.

23 Campbell, J.: Hubbard Brook Experimental Forest (USDA Forest Service): Daily Mean
24 Temperature Data, 1955 - present, <http://www.hubbardbrook.org/data/dataset.php?id=58>,
25 2014d.

26 Campbell, J. L., Bailey, A. S., Eagar, C., Green, M. B., and Battles, J. J.: Vegetation
27 treatments and hydrologic responses at the Hubbard Brook Experimental Forest, New
28 Hampshire, in: *Long-term silvicultural & ecological studies: Results for science and
29 management*, Volume 2, Yale University, Global Institute of Sustainable Forestry, Research
30 Paper 013: 011-019, 2013.

31 Camporese, M., Daly, E., and Paniconi, C.: Catchment-scale Richards equation-based
32 modeling of evapotranspiration via boundary condition switching and root water uptake
33 schemes, *Water Resources Research*, 51, 5756-5771, 10.1002/2015WR017139, 2015.

34 Cassiani, G., Boaga, J., Vanella, D., Perri, M. T., and Consoli, S.: Monitoring and modelling
35 of soil-plant interactions: the joint use of ERT, sap flow and eddy covariance data to
36 characterize the volume of an orange tree root zone, *Hydrol. Earth Syst. Sci.*, 19, 2213-2225,
37 10.5194/hess-19-2213-2015, 2015.

38 Ceola, S., Arheimer, B., Baratti, E., Blöschl, G., Capell, R., Castellarin, A., Freer, J., Han, D.,
39 Hrachowitz, M., Hundecha, Y., Hutton, C., Lindström, G., Montanari, A., Nijzink, R.,
40 Parajka, J., Toth, E., Viglione, A., and Wagener, T.: Virtual laboratories: new opportunities
41 for collaborative water science, *Hydrol. Earth Syst. Sci.*, 19, 2101-2117, 10.5194/hess-19-
42 2101-2015, 2015.

1 Dahlgren, R. A., and Driscoll, C. T.: The effects of whole-tree clear-cutting on soil processes
2 at the Hubbard Brook Experimental Forest, New Hampshire, USA, *Plant and Soil*, 158, 239-
3 262, 10.1007/BF00009499, 1994.

4 Daly, C., and McKee, W.: Meteorological data from benchmark stations at the Andrews
5 Experimental Forest, 1957 to present. Long-Term Ecological Research. Forest Science Data
6 Bank, <http://andrewsforest.oregonstate.edu/data/abstract.cfm?dbcode=MS001> 2016.

7 de Boer-Euser, T., McMillan, H. K., Hrachowitz, M., Winsemius, H. C., and Savenije, H. H.
8 G.: Influence of soil and climate on root zone storage capacity, *Water Resources Research*,
9 n/a-n/a, 10.1002/2015WR018115, 2016.

10 Donohue, R. J., Roderick, M. L., and McVicar, T. R.: On the importance of including
11 vegetation dynamics in Budyko's hydrological model, *Hydrology and Earth System Sciences
Discussions*, 11, 983-995, 2007.

13 Donohue, R. J., Roderick, M. L., and McVicar, T. R.: Roots, storms and soil pores:
14 Incorporating key ecohydrological processes into Budyko's hydrological model, *Journal of
Hydrology*, 436-437, 35-50, <http://dx.doi.org/10.1016/j.jhydrol.2012.02.033>, 2012.

16 Douglass, J. E.: THE POTENTIAL FOR WATER YIELD AUGMENTATION FROM
17 FOREST MANAGEMENT IN THE EASTERN UNITED STATES1, *JAWRA Journal of the
American Water Resources Association*, 19, 351-358, 10.1111/j.1752-1688.1983.tb04592.x,
19 1983.

20 Du, E., Link, T. E., Wei, L., and Marshall, J. D.: Evaluating hydrologic effects of spatial and
21 temporal patterns of forest canopy change using numerical modelling, *Hydrological
Processes*, 30, 217-231, 10.1002/hyp.10591, 2016.

23 Dyrness, C.: Hydrologic properties of soils on three small watersheds in the western Cascades
24 of Oregon, Res. Note PNW-111, US Department of Agriculture, Forest Service, Pacific
25 Northwest Forest and Range Experiment Station: Portland, OR, 17, 1969.

26 Eagleson, P. S.: Climate, soil, and vegetation: 3. A simplified model of soil moisture
27 movement in the liquid phase, *Water Resources Research*, 14, 722-730,
28 10.1029/WR014i005p00722, 1978.

29 Eagleson, P. S.: Ecological optimality in water-limited natural soil-vegetation systems: 1.
30 Theory and hypothesis, *Water Resources Research*, 18, 325-340,
31 10.1029/WR018i002p00325, 1982.

32 Ehret, U., Gupta, H. V., Sivapalan, M., Weijs, S. V., Schymanski, S. J., Blöschl, G., Gelfan,
33 A. N., Harman, C., Kleidon, A., Bogaard, T. A., Wang, D., Wagener, T., Scherer, U., Zehe,
34 E., Bierkens, M. F. P., Di Baldassarre, G., Parajka, J., van Beek, L. P. H., van Griensven, A.,
35 Westhoff, M. C., and Winsemius, H. C.: Advancing catchment hydrology to deal with
36 predictions under change, *Hydrol. Earth Syst. Sci.*, 18, 649-671, 10.5194/hess-18-649-2014,
37 2014.

38 Elliott, K. J., Caldwell, P. V., Brantley, S. T., Miniat, C. F., Vose, J. M., and Swank, W. T.:
39 Water yield following forest-grass-forest transitions, *Hydrol. Earth Syst. Sci. Discuss.*, 2016,
40 1-53, 10.5194/hess-2016-548, 2016.

41 Euser, T., Winsemius, H. C., Hrachowitz, M., Fenicia, F., Uhlenbrook, S., and Savenije, H. H.
42 G.: A framework to assess the realism of model structures using hydrological signatures,
43 *Hydrol. Earth Syst. Sci.*, 17, 1893-1912, 10.5194/hess-17-1893-2013, 2013.

1 Euser, T., Hrachowitz, M., Winsemius, H. C., and Savenije, H. H. G.: The effect of forcing
2 and landscape distribution on performance and consistency of model structures, *Hydrological
3 Processes*, 29, 3727-3743, 10.1002/hyp.10445, 2015.

4 Fatichi, S., Pappas, C., and Ivanov, V. Y.: Modeling plant–water interactions: an
5 ecohydrological overview from the cell to the global scale, *Wiley Interdisciplinary Reviews: Water*, 3, 327-368, 10.1002/wat2.1125, 2016.

7 Feddes, R. A., Kowalik, P. J., and Zaradny, H.: Simulation of field water use and crop yield,
8 Centre for Agricultural Publishing and Documentation., 1978.

9 Federer, A. C., Flynn, L. D., Martin, W. C., Hornbeck, J. W., and Pierce, R. S.: Thirty years
10 of hydrometeorologic data at the Hubbard Brook Experiment Forest, New Hampshire, 1990.

11 Fenicia, F., Savenije, H. H. G., Matgen, P., and Pfister, L.: Is the groundwater reservoir
12 linear? Learning from data in hydrological modelling, *Hydrol. Earth Syst. Sci.*, 10, 139-150,
13 10.5194/hess-10-139-2006, 2006.

14 Fenicia, F., Savenije, H. H. G., Matgen, P., and Pfister, L.: Understanding catchment behavior
15 through stepwise model concept improvement, *Water Resources Research*, 44, n/a-n/a,
16 10.1029/2006WR005563, 2008.

17 Fenicia, F., Savenije, H. H. G., and Avdeeva, Y.: Anomaly in the rainfall-runoff behaviour of
18 the Meuse catchment. Climate, land-use, or land-use management?, *Hydrol. Earth Syst. Sci.*,
19 13, 1727-1737, 10.5194/hess-13-1727-2009, 2009.

20 Freer, J., Beven, K., and Ambroise, B.: Bayesian Estimation of Uncertainty in Runoff
21 Prediction and the Value of Data: An Application of the GLUE Approach, *Water Resources
22 Research*, 32, 2161-2173, 10.1029/95WR03723, 1996.

23 Gao, H., Hrachowitz, M., Schymanski, S. J., Fenicia, F., Sriwongsitanon, N., and Savenije, H.
24 H. G.: Climate controls how ecosystems size the root zone storage capacity at catchment
25 scale, *Geophysical Research Letters*, 41, 7916-7923, 10.1002/2014GL061668, 2014.

26 Gentine, P., D'Odorico, P., Lintner, B. R., Sivandran, G., and Salvucci, G.: Interdependence
27 of climate, soil, and vegetation as constrained by the Budyko curve, *Geophysical Research
28 Letters*, 39, n/a-n/a, 10.1029/2012GL053492, 2012.

29 Gerrits, A. M. J., Pfister, L., and Savenije, H. H. G.: Spatial and temporal variability of
30 canopy and forest floor interception in a beech forest, *Hydrological Processes*, 24, 3011-3025,
31 10.1002/hyp.7712, 2010.

32 Gumbel, E. J.: The Return Period of Flood Flows, *The Annals of Mathematical Statistics*, 12,
33 163-190, 1941.

34 Gupta, H. V., Kling, H., Yilmaz, K. K., and Martinez, G. F.: Decomposition of the mean
35 squared error and NSE performance criteria: Implications for improving hydrological
36 modelling, *Journal of Hydrology*, 377, 80-91, <http://dx.doi.org/10.1016/j.jhydrol.2009.08.003>,
37 2009.

38 Hargreaves, G. H., and Samani, Z. A.: Reference Crop Evapotranspiration from Temperature,
39 Applied Engineering in Agriculture, 1, 96-99, 10.13031/2013.26773, 1985.

40 Harr, R. D., Harper, W. C., Krygier, J. T., and Hsieh, F. S.: Changes in storm hydrographs
41 after road building and clear-cutting in the Oregon Coast Range, *Water Resources Research*,
42 11, 436-444, 10.1029/WR011i003p00436, 1975.

1 Hornbeck, J. W., Pierce, R. S., and Federer, C. A.: Streamflow Changes after Forest Clearing
2 in New England, *Water Resources Research*, 6, 1124-1132, 10.1029/WR006i004p01124,
3 1970.

4 Hornbeck, J. W.: Storm flow from hardwood-forested and cleared watersheds in New
5 Hampshire, *Water Resources Research*, 9, 346-354, 10.1029/WR009i002p00346, 1973.

6 Hornbeck, J. W., Martin, C. W., and Eagar, C.: Summary of water yield experiments at
7 Hubbard Brook Experimental Forest, New Hampshire, *Canadian Journal of Forest Research*,
8 27, 2043-2052, 10.1139/x97-173, 1997.

9 Hornbeck, J. W., Eagar, C., Bailey, A., and Campbell, J. L.: Comparisons with results from
10 the Hubbard Brook Experimental Forest in the Northern Appalachians, *Long-Term Response*
11 of a Forest Watershed Ecosystem: Clearcutting in the Southern Appalachians, 213, 2014.

12 Hrachowitz, M., Savenije, H. H. G., Blöschl, G., McDonnell, J. J., Sivapalan, M., Pomeroy, J.
13 W., Arheimer, B., Blume, T., Clark, M. P., Ehret, U., Fenicia, F., Freer, J. E., Gelfan, A.,
14 Gupta, H. V., Hughes, D. A., Hut, R. W., Montanari, A., Pande, S., Tetzlaff, D., Troch, P. A.,
15 Uhlenbrook, S., Wagener, T., Winsemius, H. C., Woods, R. A., Zehe, E., and Cudennec, C.:
16 A decade of Predictions in Ungauged Basins (PUB)—a review, *Hydrological Sciences*
17 *Journal*, 58, 1198-1255, 10.1080/02626667.2013.803183, 2013.

18 Hrachowitz, M., Fovet, O., Ruiz, L., Euser, T., Gharari, S., Nijzink, R., Freer, J., Savenije, H.
19 H. G., and Gascuel-Odoux, C.: Process consistency in models: The importance of system
20 signatures, expert knowledge, and process complexity, *Water Resources Research*, 50, 7445-
21 7469, 10.1002/2014WR015484, 2014.

22 Hughes, J. W., and Fahey, T. J.: Colonization Dynamics of Herbs and Shrubs in a Disturbed
23 Northern Hardwood Forest, *Journal of Ecology*, 79, 605-616, 10.2307/2260656, 1991.

24 Ivanov, V. Y., Bras, R. L., and Vivoni, E. R.: Vegetation-hydrology dynamics in complex
25 terrain of semiarid areas: 1. A mechanistic approach to modeling dynamic feedbacks, *Water*
26 *Resources Research*, 44, n/a-n/a, 10.1029/2006WR005588, 2008.

27 Jobbágy, E. G., and Jackson, R. B.: Groundwater use and salinization with grassland
28 afforestation, *Global Change Biology*, 10, 1299-1312, 10.1111/j.1365-2486.2004.00806.x,
29 2004.

30 Johnson, C. E., Johnson, A. H., Huntington, T. G., and Siccama, T. G.: Whole-Tree Clear-
31 Cutting Effects on Soil Horizons and Organic-Matter Pools, *Soil Science Society of America*
32 *Journal*, 55, 497-502, 10.2136/sssaj1991.03615995005500020034x, 1991.

33 Johnson, S., and Rothacher, J.: Stream discharge in gaged watersheds at the Andrews
34 Experimental Forest, 1949 to present. *Long-Term Ecological Research*.Forest Science Data
35 Bank, Forest Science Data Bank,
36 <http://andrewsforest.oregonstate.edu/data/abstract.cfm?dbcode=HF004> 2016.

37 Jones, J. A., and Grant, G. E.: Peak Flow Responses to Clear-Cutting and Roads in Small and
38 Large Basins, Western Cascades, Oregon, *Water Resources Research*, 32, 959-974,
39 10.1029/95WR03493, 1996.

40 Jones, J. A., and Post, D. A.: Seasonal and successional streamflow response to forest cutting
41 and regrowth in the northwest and eastern United States, *Water Resources Research*, 40, n/a-
42 n/a, 10.1029/2003WR002952, 2004.

43 Jothiyangkoon, C., Sivapalan, M., and Farmer, D. L.: Process controls of water balance
44 variability in a large semi-arid catchment: downward approach to hydrological model

1 development, *Journal of Hydrology*, 254, 174-198, [http://dx.doi.org/10.1016/S0022-1694\(01\)00496-6](http://dx.doi.org/10.1016/S0022-1694(01)00496-6), 2001.

3 Kleidon, A.: Global Datasets of Rooting Zone Depth Inferred from Inverse Methods, *Journal*
4 of *Climate*, 17, 2714-2722, 10.1175/1520-0442(2004)017<2714:GDORZD>2.0.CO;2, 2004.

5 Kuczera, G.: Prediction of water yield reductions following a bushfire in ash-mixed species
6 eucalypt forest, *Journal of Hydrology*, 94, 215-236, [http://dx.doi.org/10.1016/0022-1694\(87\)90054-0](http://dx.doi.org/10.1016/0022-1694(87)90054-0), 1987.

8 Laio, F., Porporato, A., Ridolfi, L., and Rodriguez-Iturbe, I.: Plants in water-controlled
9 ecosystems: active role in hydrologic processes and response to water stress: II. Probabilistic
10 soil moisture dynamics, *Advances in Water Resources*, 24, 707-723,
11 [http://dx.doi.org/10.1016/S0309-1708\(01\)00005-7](http://dx.doi.org/10.1016/S0309-1708(01)00005-7), 2001.

12 Legesse, D., Vallet-Coulob, C., and Gasse, F.: Hydrological response of a catchment to
13 climate and land use changes in Tropical Africa: case study South Central Ethiopia, *Journal of*
14 *Hydrology*, 275, 67-85, [http://dx.doi.org/10.1016/S0022-1694\(03\)00019-2](http://dx.doi.org/10.1016/S0022-1694(03)00019-2), 2003.

15 Li, K. Y., Coe, M. T., Ramankutty, N., and Jong, R. D.: Modeling the hydrological impact of
16 land-use change in West Africa, *Journal of Hydrology*, 337, 258-268,
17 <http://dx.doi.org/10.1016/j.jhydrol.2007.01.038>, 2007.

18 Liancourt, P., Sharkhuu, A., Ariuntsetseg, L., Boldgiv, B., Helliker, B. R., Plante, A. F.,
19 Petraitis, P. S., and Casper, B. B.: Temporal and spatial variation in how vegetation alters the
20 soil moisture response to climate manipulation, *Plant and Soil*, 351, 249-261,
21 10.1007/s11104-011-0956-y, 2012.

22 Likens, G. E., Bormann, F. H., Johnson, N. M., Fisher, D. W., and Pierce, R. S.: Effects of
23 Forest Cutting and Herbicide Treatment on Nutrient Budgets in the Hubbard Brook
24 Watershed-Ecosystem, *Ecological Monographs*, 40, 23-47, 10.2307/1942440, 1970.

25 Likens, G. E.: *Biogeochemistry of a forested ecosystem*, Springer, New York, 2013.

26 Lindström, G., Pers, C., Rosberg, J., Strömqvist, J., and Arheimer, B.: Development and
27 testing of the HYPE (Hydrological Predictions for the Environment) water quality model for
28 different spatial scales, *Hydrology Research*, 41, 295-319, 10.2166/nh.2010.007, 2010.

29 Mahe, G., Paturel, J.-E., Servat, E., Conway, D., and Dezetter, A.: The impact of land use
30 change on soil water holding capacity and river flow modelling in the Nakambe River,
31 Burkina-Faso, *Journal of Hydrology*, 300, 33-43,
32 <http://dx.doi.org/10.1016/j.jhydrol.2004.04.028>, 2005.

33 Martin, C. W.: Soil disturbance by logging in New England--review and management
34 recommendations, *Northern Journal of Applied Forestry*, 5, 30-34, 1988.

35 Martin, C. W., Hornbeck, J. W., Likens, G. E., and Buso, D. C.: Impacts of intensive
36 harvesting on hydrology and nutrient dynamics of northern hardwood forests, *Canadian*
37 *Journal of Fisheries and Aquatic Sciences*, 57, 19-29, 10.1139/f00-106, 2000.

38 McDowell, N., Pockman, W. T., Allen, C. D., Breshears, D. D., Cobb, N., Kolb, T., Plaut, J.,
39 Sperry, J., West, A., Williams, D. G., and Yepez, E. A.: Mechanisms of plant survival and
40 mortality during drought: why do some plants survive while others succumb to drought?, *New*
41 *Phytologist*, 178, 719-739, 10.1111/j.1469-8137.2008.02436.x, 2008.

1 Mencuccini, M.: The ecological significance of long-distance water transport: short-term
2 regulation, long-term acclimation and the hydraulic costs of stature across plant life forms,
3 *Plant, Cell & Environment*, 26, 163-182, 10.1046/j.1365-3040.2003.00991.x, 2003.

4 Milly, P. C. D.: Climate, soil water storage, and the average annual water balance, *Water
5 Resources Research*, 30, 2143-2156, 10.1029/94WR00586, 1994.

6 Milly, P. C. D., and Dunne, K. A.: Sensitivity of the Global Water Cycle to the Water-
7 Holding Capacity of Land, *Journal of Climate*, 7, 506-526, doi:10.1175/1520-
8 0442(1994)007<0506:SOTGWC>2.0.CO;2, 1994.

9 Montanari, A., and Toth, E.: Calibration of hydrological models in the spectral domain: An
10 opportunity for scarcely gauged basins?, *Water Resources Research*, 43, n/a-n/a,
11 10.1029/2006WR005184, 2007.

12 Montanari, A., Young, G., Savenije, H. H. G., Hughes, D., Wagener, T., Ren, L. L.,
13 Koutsoyiannis, D., Cudennec, C., Toth, E., Grimaldi, S., Blöschl, G., Sivapalan, M., Beven,
14 K., Gupta, H., Hipsey, M., Schaeefli, B., Arheimer, B., Boegh, E., Schymanski, S. J., Di
15 Baldassarre, G., Yu, B., Hubert, P., Huang, Y., Schumann, A., Post, D. A., Srinivasan, V.,
16 Harman, C., Thompson, S., Rogger, M., Viglione, A., McMillan, H., Characklis, G., Pang, Z.,
17 and Belyaev, V.: "Panta Rhei—Everything Flows": Change in hydrology and society—The
18 IAHS Scientific Decade 2013–2022, *Hydrological Sciences Journal*, 58, 1256-1275,
19 10.1080/02626667.2013.809088, 2013.

20 Mou, P., Fahey, T. J., and Hughes, J. W.: Effects of Soil Disturbance on Vegetation Recovery
21 and Nutrient Accumulation Following Whole-Tree Harvest of a Northern Hardwood
22 Ecosystem, *Journal of Applied Ecology*, 30, 661-675, 10.2307/2404245, 1993.

23 Nash, J. E., and Sutcliffe, J. V.: River flow forecasting through conceptual models part I — A
24 discussion of principles, *Journal of Hydrology*, 10, 282-290, [http://dx.doi.org/10.1016/0022-1694\(70\)90255-6](http://dx.doi.org/10.1016/0022-1694(70)90255-6), 1970.

26 Nijzink, R. C., Samaniego, L., Mai, J., Kumar, R., Thober, S., Zink, M., Schäfer, D., Savenije,
27 H. H. G., and Hrachowitz, M.: The importance of topography-controlled sub-grid process
28 heterogeneity and semi-quantitative prior constraints in distributed hydrological models,
29 *Hydrol. Earth Syst. Sci.*, 20, 1151-1176, 10.5194/hess-20-1151-2016, 2016.

30 Nobel, P. S., and Cui, M.: Hydraulic Conductances of the Soil, the Root-Soil Air Gap, and the
31 Root: Changes for Desert Succulents in Drying Soil, *Journal of Experimental Botany*, 43,
32 319-326, 10.1093/jxb/43.3.319, 1992.

33 North, G. B., and Nobel, P. S.: Drought-induced changes in hydraulic conductivity and
34 structure in roots of Ferocactus acanthodes and Opuntia ficus-indica, *New Phytologist*, 120,
35 9-19, 10.1111/j.1469-8137.1992.tb01053.x, 1992.

36 Onstad, C. A., and Jamieson, D. G.: Modeling the Effect of Land Use Modifications on
37 Runoff, *Water Resources Research*, 6, 1287-1295, 10.1029/WR006i005p01287, 1970.

38 Oudin, L., Andréassian, V., Perrin, C., and Anctil, F.: Locating the sources of low-pass
39 behavior within rainfall-runoff models, *Water Resources Research*, 40, n/a-n/a,
40 10.1029/2004WR003291, 2004.

41 Parajka, J., Merz, R., and Blöschl, G.: Uncertainty and multiple objective calibration in
42 regional water balance modelling: case study in 320 Austrian catchments, *Hydrological
43 Processes*, 21, 435-446, 10.1002/hyp.6253, 2007.

1 Patric, J. H., and Reinhart, K. G.: Hydrologic Effects of Deforesting Two Mountain
2 Watersheds in West Virginia, *Water Resources Research*, 7, 1182-1188,
3 10.1029/WR007i005p01182, 1971.

4 Perrin, C., Michel, C., and Andréassian, V.: Improvement of a parsimonious model for
5 streamflow simulation, *Journal of Hydrology*, 279, 275-289, [http://dx.doi.org/10.1016/S0022-1694\(03\)00225-7](http://dx.doi.org/10.1016/S0022-1694(03)00225-7), 2003.

7 Porporato, A., Daly, E., Rodriguez, x, Iturbe, I., and Associate Editor: William, F. F.: Soil
8 Water Balance and Ecosystem Response to Climate Change, *The American Naturalist*, 164,
9 625-632, 10.1086/424970, 2004.

10 Refsgaard, J. C., and Storm, B.: MIKE SHE, in: *Computer Models of Watershed Hydrology*,
11 edited by: Singh, V. J., Water Resour. Publ., Littleton, Colorado, 1995.

12 Reynolds, J. F., Kemp, P. R., and Tenhunen, J. D.: Effects of long-term rainfall variability on
13 evapotranspiration and soil water distribution in the Chihuahuan Desert: A modeling analysis,
14 *Plant Ecology*, 150, 145-159, 10.1023/a:1026530522612, 2000.

15 Rodriguez-Iturbe, I.: Ecohydrology: A hydrologic perspective of climate-soil-vegetation
16 dynamics, *Water Resources Research*, 36, 3-9, 10.1029/1999WR900210, 2000.

17 Rodriguez-Iturbe, I., D'Odorico, P., Laio, F., Ridolfi, L., and Tamea, S.: Challenges in humid
18 land ecohydrology: Interactions of water table and unsaturated zone with climate, soil, and
19 vegetation, *Water Resources Research*, 43, n/a-n/a, 10.1029/2007WR006073, 2007.

20 Rood, S. B., Braatne, J. H., and Hughes, F. M. R.: Ecophysiology of riparian cottonwoods:
21 stream flow dependency, water relations and restoration, *Tree Physiology*, 23, 1113-1124,
22 10.1093/treephys/23.16.1113, 2003.

23 Rothacher, J.: Streamflow from small watersheds on the western slope of the Cascade Range
24 of Oregon, *Water Resources Research*, 1, 125-134, 10.1029/WR001i001p00125, 1965.

25 Rothacher, J., Dyrness, C. T., Fredriksen, R. L., Forest, P. N., and Station, R. E.: Hydrologic
26 and related characteristics of three small watersheds in the Oregon Cascades, Pacific
27 Northwest Forest and Range Experiment Station, U.S. Dept. of Agriculture, 1967.

28 Rothacher, J.: Increases in Water Yield Following Clear-Cut Logging in the Pacific
29 Northwest, *Water Resources Research*, 6, 653-658, 10.1029/WR006i002p00653, 1970.

30 Schenk, H. J., and Jackson, R. B.: Rooting depths, lateral root spreads and below-
31 ground/above-ground allometries of plants in water-limited ecosystems, *Journal of Ecology*,
32 90, 480-494, 10.1046/j.1365-2745.2002.00682.x, 2002.

33 Schoups, G., Hopmans, J. W., Young, C. A., Vrugt, J. A., and Wallender, W. W.: Multi-
34 criteria optimization of a regional spatially-distributed subsurface water flow model, *Journal
35 of Hydrology*, 311, 20-48, <http://dx.doi.org/10.1016/j.jhydrol.2005.01.001>, 2005.

36 Schymanski, S. J., Sivapalan, M., Roderick, M. L., Beringer, J., and Hutley, L. B.: An
37 optimality-based model of the coupled soil moisture and root dynamics, *Hydrology and Earth
38 System Sciences Discussions*, 12, 913-932, 2008.

39 Seibert, J., and McDonnell, J. J.: Land-cover impacts on streamflow: a change-detection
40 modelling approach that incorporates parameter uncertainty, *Hydrological Sciences Journal*,
41 55, 316-332, 10.1080/02626661003683264, 2010.

1 Seibert, J., McDonnell, J. J., and Woodsmith, R. D.: Effects of wildfire on catchment runoff
2 response: a modelling approach to detect changes in snow-dominated forested catchments,
3 *Hydrology Research*, 41, 378-390, 2010.

4 Seneviratne, S. I., Corti, T., Davin, E. L., Hirschi, M., Jaeger, E. B., Lehner, I., Orlowsky, B.,
5 and Teuling, A. J.: Investigating soil moisture–climate interactions in a changing climate: A
6 review, *Earth-Science Reviews*, 99, 125-161,
7 <http://dx.doi.org/10.1016/j.earscirev.2010.02.004>, 2010.

8 Seneviratne, S. I., Wilhelm, M., Stanelle, T., van den Hurk, B., Hagemann, S., Berg, A.,
9 Cheruy, F., Higgins, M. E., Meier, A., Brovkin, V., Claussen, M., Ducharne, A., Dufresne, J.-
10 L., Findell, K. L., Ghattas, J., Lawrence, D. M., Malyshev, S., Rummukainen, M., and Smith,
11 B.: Impact of soil moisture–climate feedbacks on CMIP5 projections: First results from the
12 GLACE-CMIP5 experiment, *Geophysical Research Letters*, 40, 5212-5217,
13 10.1002/grl.50956, 2013.

14 Shamir, E., Imam, B., Morin, E., Gupta, H. V., and Sorooshian, S.: The role of hydrograph
15 indices in parameter estimation of rainfall–runoff models, *Hydrological Processes*, 19, 2187-
16 2207, 10.1002/hyp.5676, 2005.

17 Sivapalan, M., Blöschl, G., Zhang, L., and Vertessy, R.: Downward approach to hydrological
18 prediction, *Hydrological Processes*, 17, 2101-2111, 10.1002/hyp.1425, 2003.

19 Sperry, J. S., Hacke, U. G., Oren, R., and Comstock, J. P.: Water deficits and hydraulic limits
20 to leaf water supply, *Plant, Cell & Environment*, 25, 251-263, 10.1046/j.0016-
21 8025.2001.00799.x, 2002.

22 Swift, L. W., and Swank, W. T.: Long term responses of streamflow following clearcutting
23 and regrowth / Réactions à long terme du débit des cours d'eau après coupe et repeuplement,
24 *Hydrological Sciences Bulletin*, 26, 245-256, 10.1080/02626668109490884, 1981.

25 Teuling, A. J., Van Loon, A. F., Seneviratne, S. I., Lehner, I., Aubinet, M., Heinesch, B.,
26 Bernhofer, C., Grünwald, T., Prasse, H., and Spank, U.: Evapotranspiration amplifies
27 European summer drought, *Geophysical Research Letters*, 40, 2071-2075, 10.1002/grl.50495,
28 2013.

29 Troch, P. A., Martinez, G. F., Pauwels, V. R. N., Durcik, M., Sivapalan, M., Harman, C.,
30 Brooks, P. D., Gupta, H., and Huxman, T.: Climate and vegetation water use efficiency at
31 catchment scales, *Hydrological Processes*, 23, 2409-2414, 10.1002/hyp.7358, 2009.

32 Troch, P. A., Lahmers, T., Meira, A., Mukherjee, R., Pedersen, J. W., Roy, T., and Valdés-
33 Pineda, R.: Catchment coevolution: A useful framework for improving predictions of
34 hydrological change?, *Water Resources Research*, 51, 4903-4922, 10.1002/2015WR017032,
35 2015.

36 Tron, S., Perona, P., Gorla, L., Schwarz, M., Laio, F., and Ridolfi, L.: The signature of
37 randomness in riparian plant root distributions, *Geophysical Research Letters*, 42, 7098-7106,
38 10.1002/2015GL064857, 2015.

39 Vose, J. M., Miniat, C. F., Luce, C. H., Asbjornsen, H., Caldwell, P. V., Campbell, J. L.,
40 Grant, G. E., Isaak, D. J., Loheide II, S. P., and Sun, G.: Ecohydrological implications of
41 drought for forests in the United States, *Forest Ecology and Management*,
42 <http://dx.doi.org/10.1016/j.foreco.2016.03.025>,

1 Wagener, T., Sivapalan, M., Troch, P., and Woods, R.: Catchment Classification and
2 Hydrologic Similarity, *Geography Compass*, 1, 901-931, 10.1111/j.1749-8198.2007.00039.x,
3 2007.

4 Waichler, S. R., Wemple, B. C., and Wigmosta, M. S.: Simulation of water balance and forest
5 treatment effects at the H.J. Andrews Experimental Forest, *Hydrological Processes*, 19, 3177-
6 3199, 10.1002/hyp.5841, 2005.

7 Wang-Erlandsson, L., Bastiaanssen, W. G. M., Gao, H., Jägermeyr, J., Senay, G. B., van Dijk,
8 A. I. J. M., Guerschman, J. P., Keys, P. W., Gordon, L. J., and Savenije, H. H. G.: Global root
9 zone storage capacity from satellite-based evaporation, *Hydrol. Earth Syst. Sci.*, 20, 1459-
10 1481, 10.5194/hess-20-1459-2016, 2016.

11 Weibull, W.: A Statistical Distribution Function of Wide Applicability, *Journal of applied
12 mechanics*, 18, 293-297, 1951.

13 Westerberg, I. K., Guerrero, J. L., Younger, P. M., Beven, K. J., Seibert, J., Halldin, S., Freer,
14 J. E., and Xu, C. Y.: Calibration of hydrological models using flow-duration curves, *Hydrol.
15 Earth Syst. Sci.*, 15, 2205-2227, 10.5194/hess-15-2205-2011, 2011.

16 Westra, S., Thyre, M., Leonard, M., Kavetski, D., and Lambert, M.: A strategy for diagnosing
17 and interpreting hydrological model nonstationarity, *Water Resources Research*, 50, 5090-
18 5113, 10.1002/2013WR014719, 2014.

19 Wilks, D. S.: *Statistical Methods in the Atmospheric Sciences*, Elsevier Science, 2005.

20 Yadav, M., Wagener, T., and Gupta, H.: Regionalization of constraints on expected watershed
21 response behavior for improved predictions in ungauged basins, *Advances in Water
22 Resources*, 30, 1756-1774, <http://dx.doi.org/10.1016/j.advwatres.2007.01.005>, 2007.

23 Yilmaz, K. K., Gupta, H. V., and Wagener, T.: A process-based diagnostic approach to model
24 evaluation: Application to the NWS distributed hydrologic model, *Water Resources Research*,
25 44, n/a-n/a, 10.1029/2007WR006716, 2008.

26 Zhang, S., Yang, H., Yang, D., and Jayawardena, A. W.: Quantifying the effect of vegetation
27 change on the regional water balance within the Budyko framework, *Geophysical Research
28 Letters*, 43, 1140-1148, 10.1002/2015GL066952, 2016.

29 Zhao, R.-J.: The Xinanjiang model applied in China, *Journal of Hydrology*, 135, 371-381,
30 [http://dx.doi.org/10.1016/0022-1694\(92\)90096-E](http://dx.doi.org/10.1016/0022-1694(92)90096-E), 1992.

31

1 Table 1. Overview of the catchments and their sub-catchments (WS).

Catchment	Deforestation period	Treatment	Area [km ²]	Affected Area [%]	Aridity index [-]	Precipitation n [mm/year]	Discharge [mm/year]	Potential evaporation [mm/year]
HJ Andrews WS1	1962-1966.	Burned 1966	0.956	100	0.39	2305	1361	902
HJ Andrews WS2	-	-	0.603	-	0.39	2305	1251	902
Hubbard Brook WS2	1965-1968	Herbicides	0.156	100	0.57	1471	1059	784
Hubbard Brook WS3	-	-	0.424	-	0.54	1464	951	787
Hubbard Brook WS5	1983-1984	No treatment	0.219	87	0.51	1518	993	746

2

3 Table 2. Applied parameter ranges for root zone storage derivation

Catchment	I _{max,eq} [mm]	I _{max,change} [mm]	T _r [days]
HJ Andrews WS1	1-5	0-5	0-3650
HJ Andrews WS2	1-5	-	-
Hubbard Brook WS2	1-5	5-10	0-3650
Hubbard Brook WS3	1-5	-	-
Hubbard Brook WS5	1-5	0-5	0-3650

4

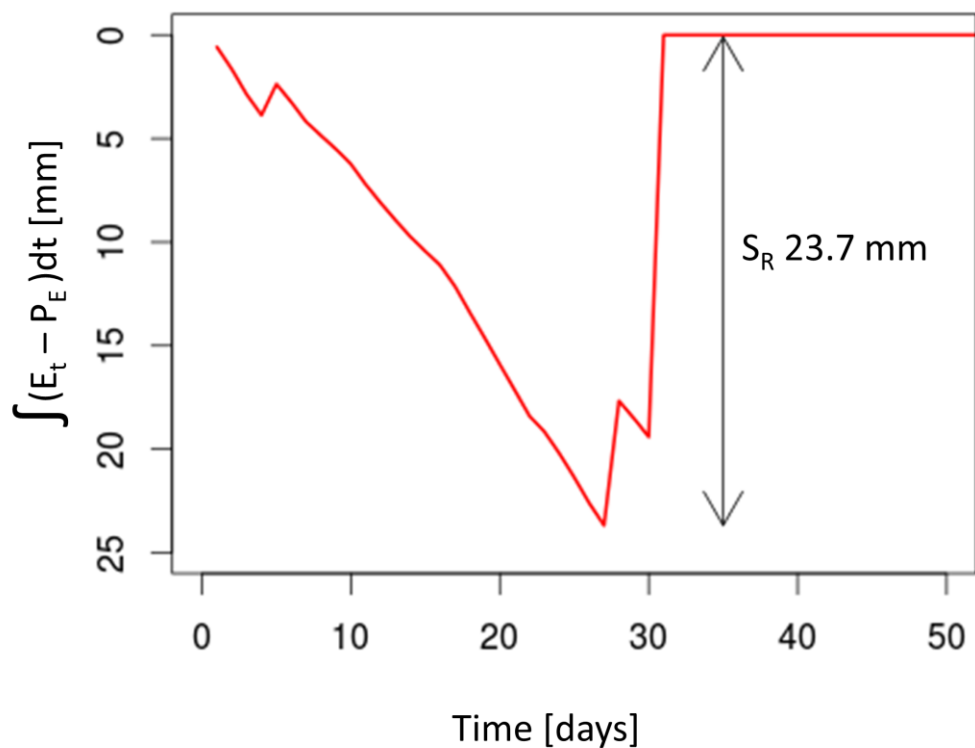
5

1 Table 3. Overview of the hydrological signatures

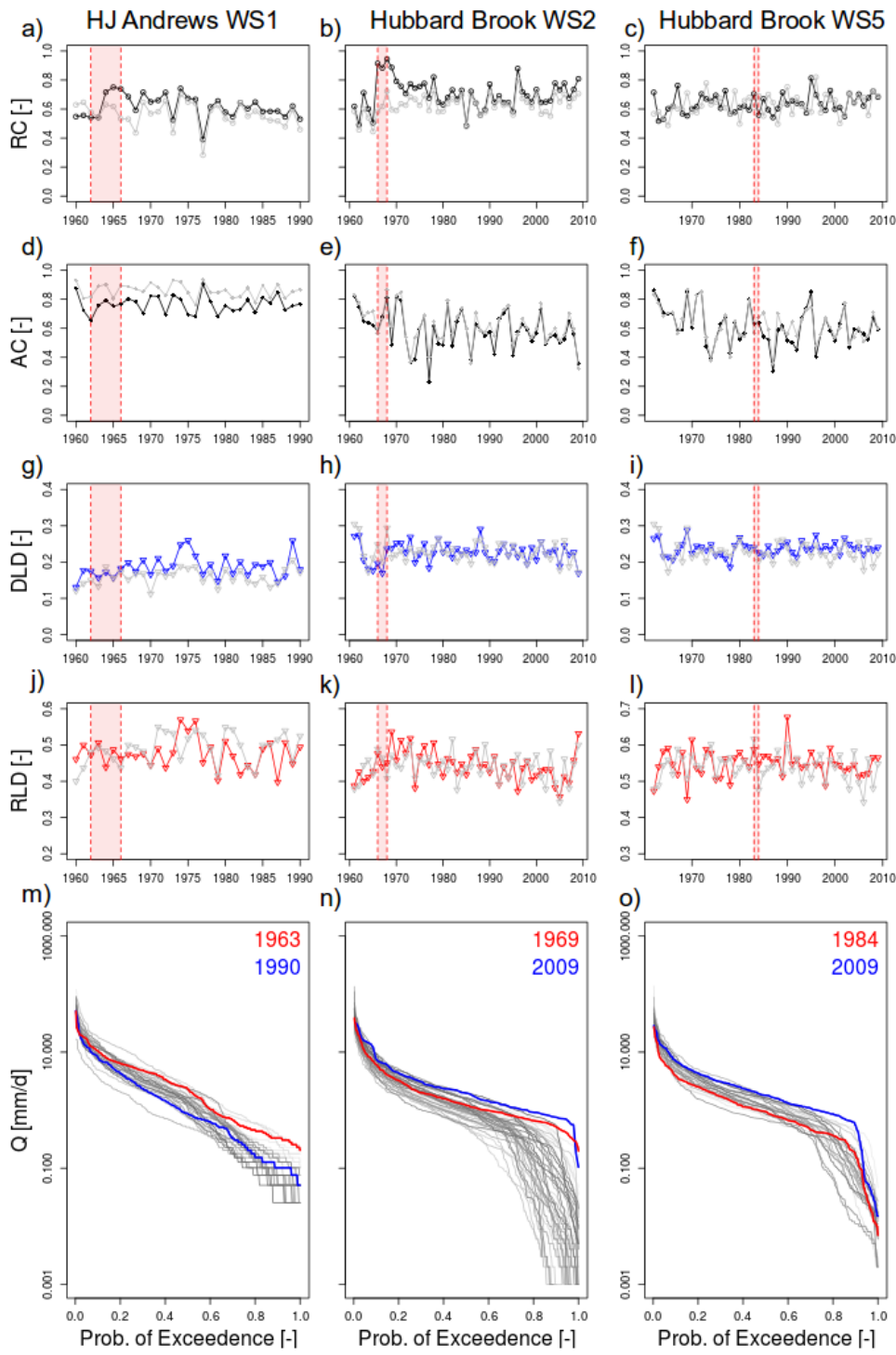
Signature	Description	Reference
S_{QMA}	Mean annual runoff	
S_{AC}	One day autocorrelation coefficient	Montanari and Toth (2007)
$S_{AC,summer}$	One day autocorrelation the summer period	Euser et al. (2013)
$S_{AC,winter}$	One day autocorrelation the winter period	Euser et al. (2013)
S_{RLD}	Rising limb density	Shamir et al. (2005)
S_{DLI}	Declining limb density	Shamir et al. (2005)
S_{Q5}	Flow exceeded in 5% of the time	Jothityangkoon et al. (2001)
S_{Q50}	Flow exceeded in 50% of the time	Jothityangkoon et al. (2001)
S_{Q95}	Flow exceeded in 95% of the time	Jothityangkoon et al. (2001)
$S_{Q5,summer}$	Flow exceeded in 5% of the summer time	Yilmaz et al. (2008)
$S_{Q50,summer}$	Flow exceeded in 50% of the summer time	Yilmaz et al. (2008)
$S_{Q95,summer}$	Flow exceeded in 95% of the summer time	Yilmaz et al. (2008)
$S_{Q5,winter}$	Flow exceeded in 5% of the winter time	Yilmaz et al. (2008)
$S_{Q50,winter}$	Flow exceeded in 50% of the winter time	Yilmaz et al. (2008)
$S_{Q95,winter}$	Flow exceeded in 95% of the winter time	Yilmaz et al. (2008)
S_{Peaks}	Peak distribution	Euser et al. (2013)
$S_{Peaks,summer}$	Peak distribution summer period	Euser et al. (2013)
$S_{Peaks,winter}$	Peak distribution winter period	Euser et al. (2013)
$S_{Qpeak,10}$	Flow exceeded in 10% of the peaks	
$S_{Qpeak,50}$	Flow exceeded in 50% of the peaks	
$S_{Qsummer,peak,10}$	Flow exceeded in 10% of the summer peaks	
$S_{Qsummer,peak,50}$	Flow exceeded in 10% of the summer peaks	
$S_{Qwinter,peak,10}$	Flow exceeded in 10% of the winter peaks	

$S_{Q_{\text{winter,peak},50}}$	Flow exceeded in 50% of the winter peaks	
S_{SFDC}	Slope flow duration curve	Yadav et al. (2007)
S_{LFR}	Low flow ratio (Q_{90}/Q_{50})	
S_{FDC}	Flow duration curve	Westerberg et al. (2011)
$S_{\text{AC,serie}}$	Autocorrelation series (200 days lag time)	Montanari and Toth (2007)

1
2



1
2 Figure 1. Derivation of root zone storage capacity (S_R) for one specific time period in the
3 Hubbard Brook WS2 catchment as difference between the cumulative transpiration (E_t) and
4 the cumulative effective precipitation (P_E).



1

2 Figure 2. Evolution of signatures in time of a-c) the runoff coefficient, d-f) the 1-day
3 autocorrelation, g-i) the declining limb density, j-l) the rising limb density with the reference
4 watersheds in grey and periods of deforestation in red shading. The flow duration curves for
5 HJ Andrews WS1, Hubbard Brook WS2 and Hubbard Brook WS5 are shown in m-o), where
6 years between the first and last year are colored from lightgray till darkgrey progressively in
7 time.

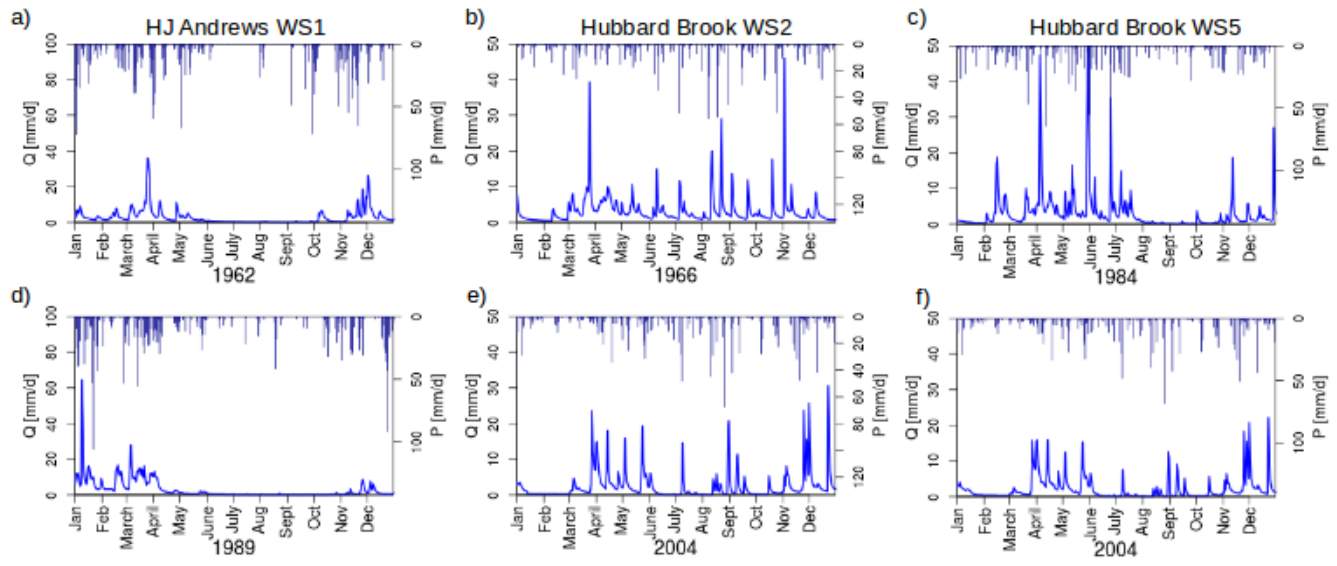
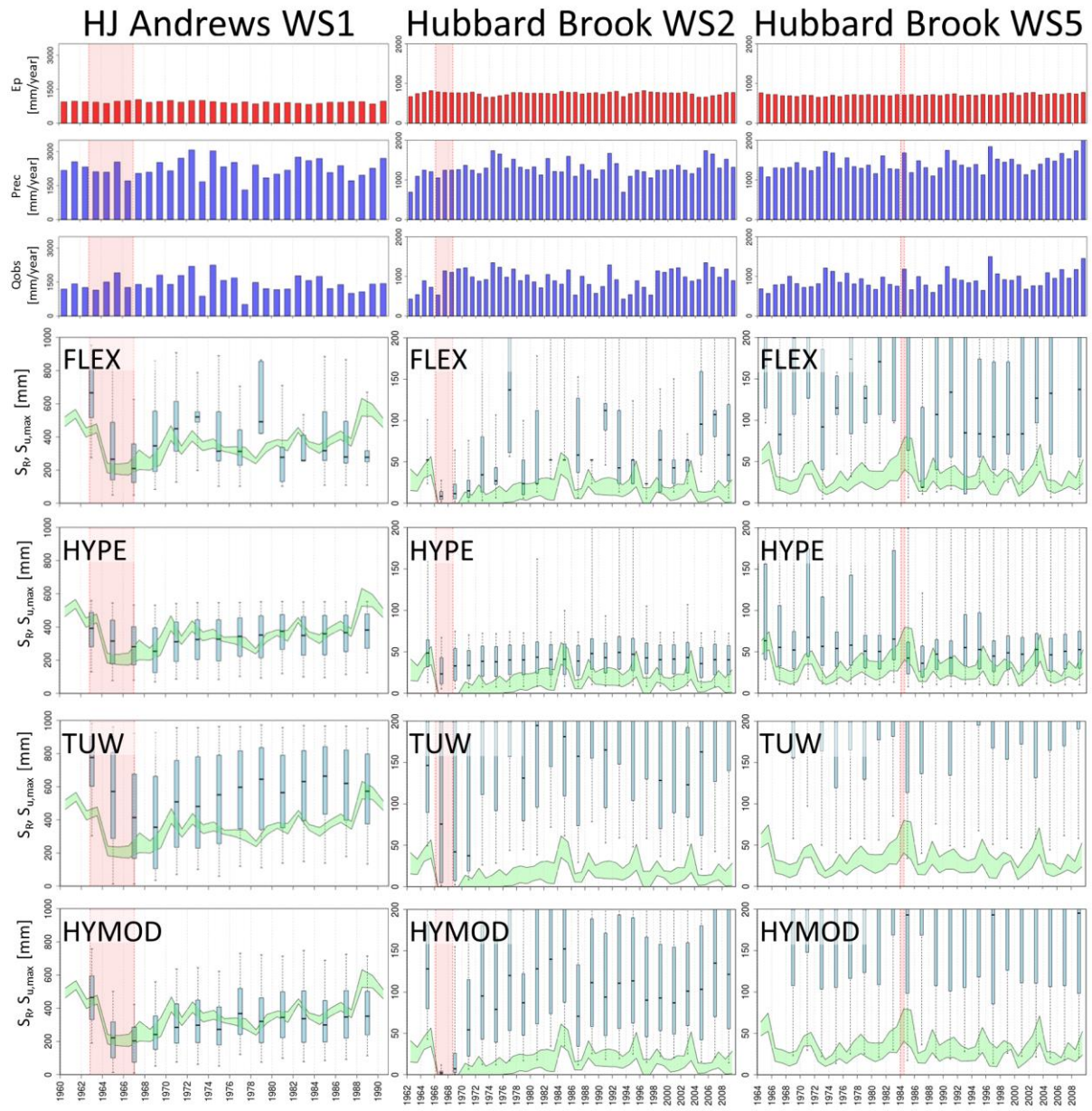
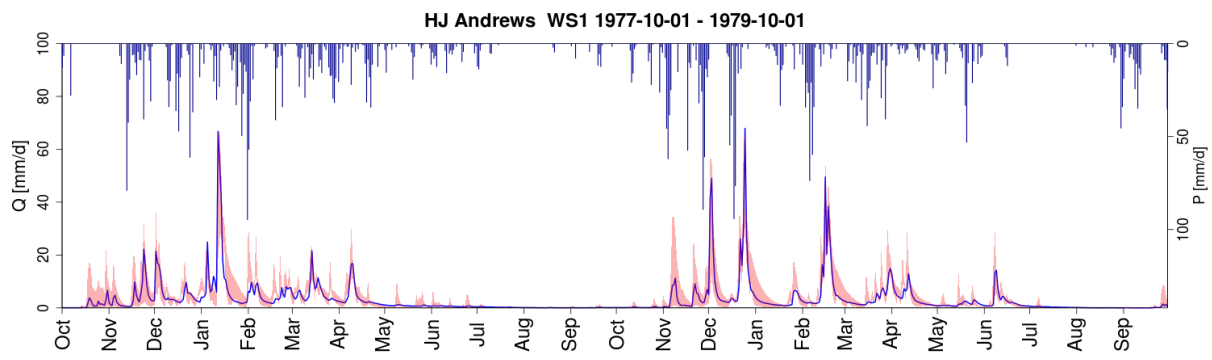


Figure 3. Hydrographs for HJ Andrews WS1 in a) 1963 (annual precipitation $P_A = 2018 \text{ mm yr}^{-1}$, $E_{p,A} = 951 \text{ mm yr}^{-1}$) and b) 1989 ($P_A = 1752 \text{ mm yr}^{-1}$, $E_{p,A} = 846 \text{ mm yr}^{-1}$), Hubbard Brook WS2 in c) 1966 ($P_A = 1222 \text{ mm yr}^{-1}$, $E_{p,A} = 788 \text{ mm yr}^{-1}$ and d) 2004 ($P_A = 1296 \text{ mm yr}^{-1}$, annual $E_{p,A} = 761 \text{ mm yr}^{-1}$ and Hubbard Brook WS5 in e) 1984 ($P_A = 1480 \text{ mm yr}^{-1}$, annual $E_{p,A} = 721 \text{ mm yr}^{-1}$) and f) 2004 ($P_A = 1311 \text{ mm yr}^{-1}$, $E_{p,A} = 731 \text{ mm yr}^{-1}$).

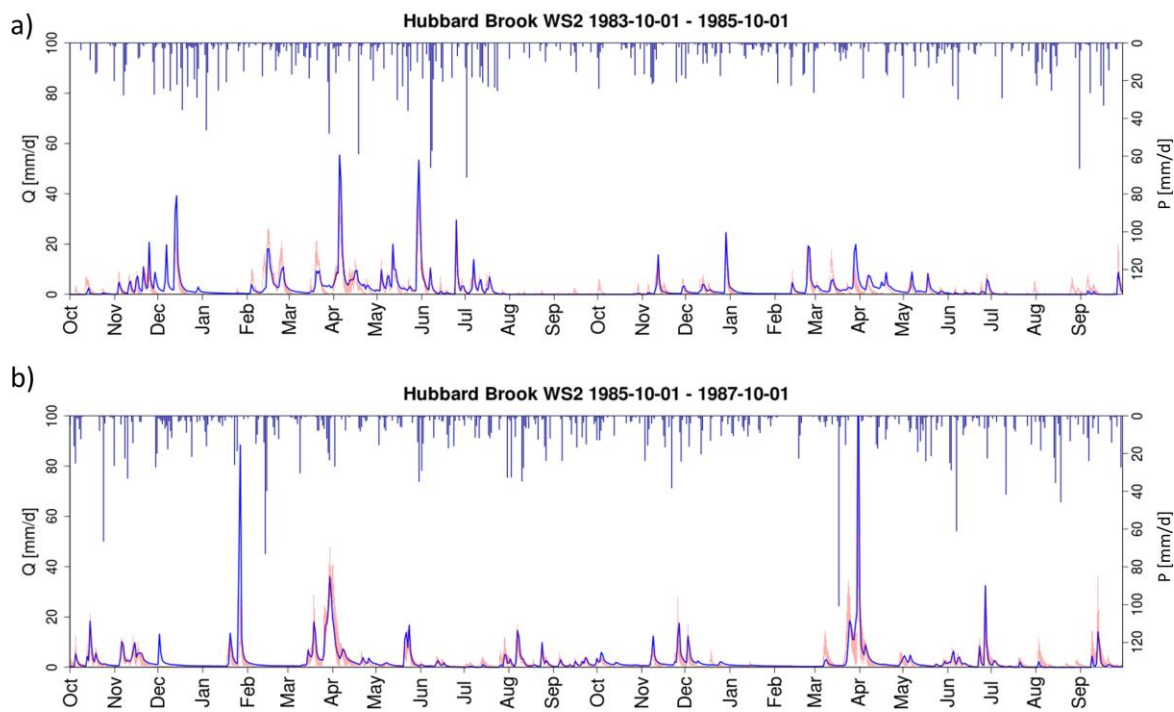


1

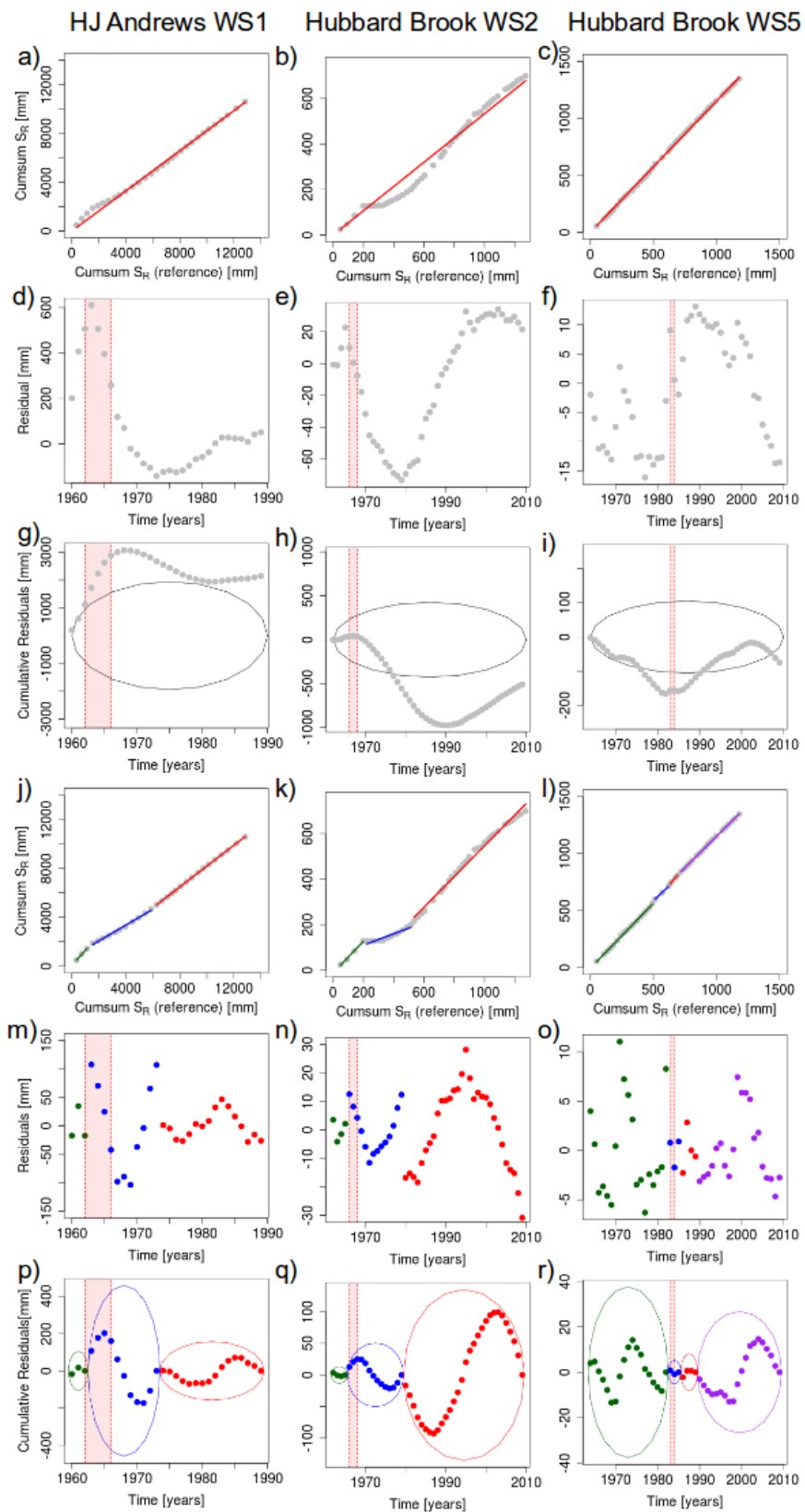
2 Figure 4. Evolution of root zone storage capacity $S_{R,1yr}$ from water balance-based estimation
 3 (green shaded area, a range of solutions due to the sampling of the unknown interception
 4 capacity) compared with $S_{u,max,2yr}$ estimates obtained from the calibration of four models
 5 (FLEX, HYPE, TUW, HYMOD; blue boxplots) for a) HJ Andrews WS1, b) Hubbard Brook
 6 WS2 and c) Hubbard Brook WS5. Red shaded areas are periods of deforestation.



1
2 Figure 5. Observed and modelled hydrograph for HJ Andrews WS1 the years of 1978 and
3 1979, with the red colored area indicating the 5/95% uncertainty intervals of the modelled
4 discharge. Blue bars show daily precipitation.

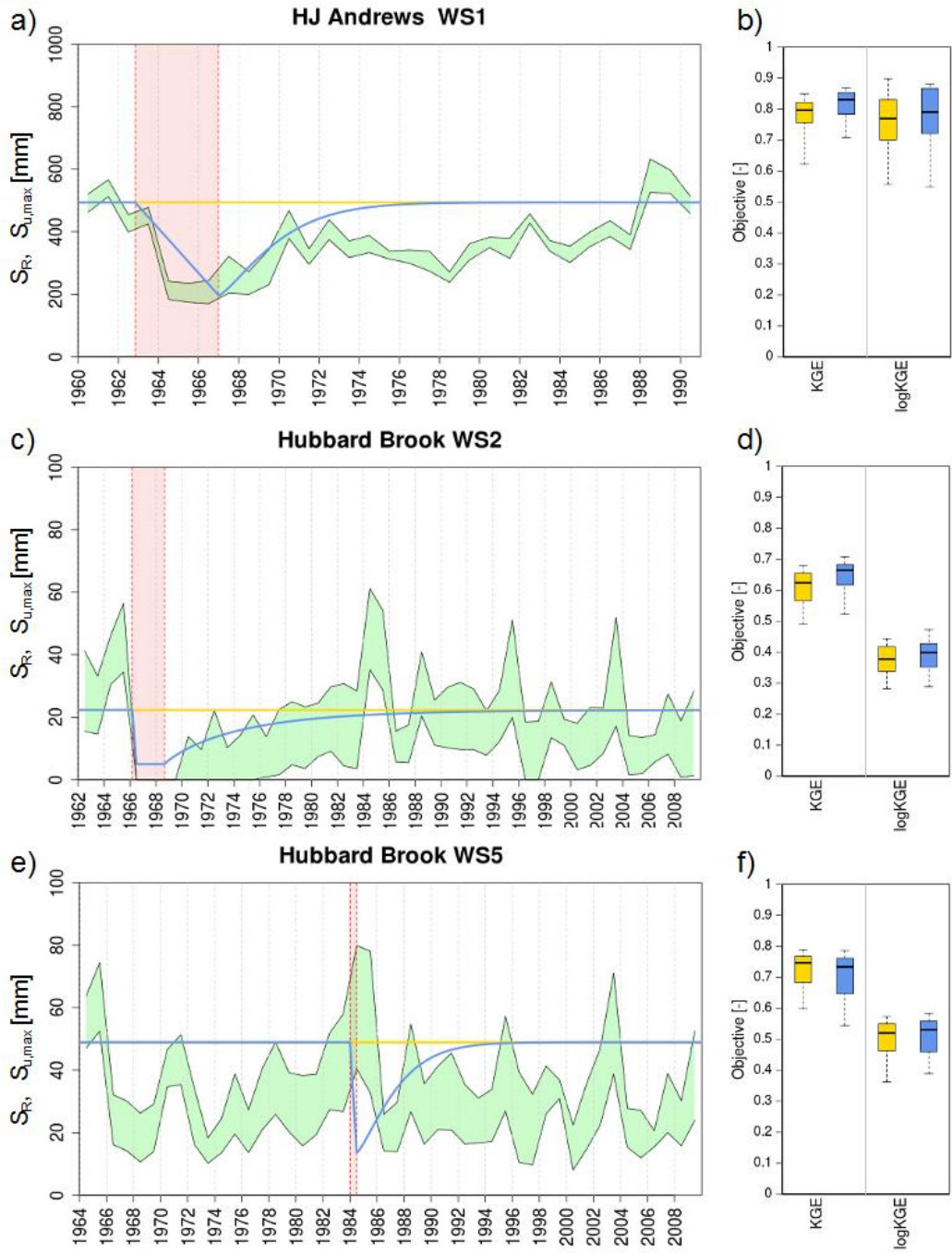


5
6 Figure 6. Observed and modelled hydrograph for Hubbard Brook WS2 for a) the years of
7 1984 and 1985 and b) the years of 1986 and 1987, with the red colored area indicating the
8 5/95% uncertainty intervals of the modelled discharge. Blue bars show daily precipitation.
9



1 Figure 7. Trend analysis for $S_{R,1yr}$ in HJ Andrews WS1, Hubbard Brook WS2 and WS5 based
2 on comparison with the control watersheds with a-c) Cumulative root zone storages ($S_{R,1yr}$)
3 with regression, d-f) residuals of the regression of cumulative root zone storages, g-i)
4 significance test; the cumulative residuals do not plot within the 95%-confidence ellipse,
5 rejecting the null-hypothesis that the two time series are homogeneous, j-l) piecewise linear
6 regression based on break points in residuals plot, m-o) residuals of piecewise linear
7 regression, p-r) significance test based on piecewise linear regression with homogeneous time
8 series of $S_{R,1yr}$. The different colors (green, blue, red, violet) indicate individual homogeneous
9 time periods.

10



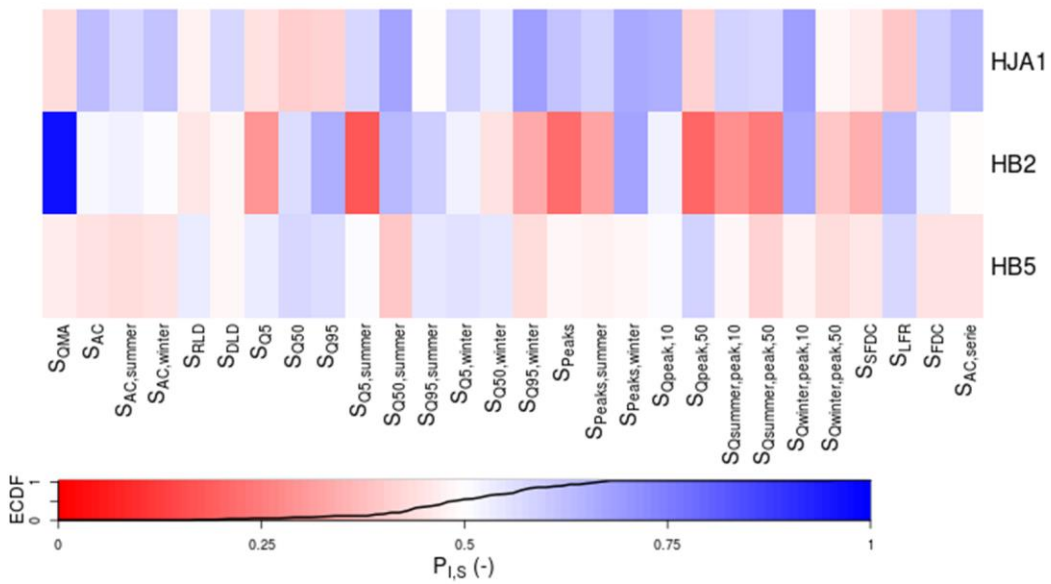
1
2 Figure 8. The time invariant $S_{u,\max}$ formulation represented by $S_{R, 20\text{yr}}$ (yellow) and time
3 dynamic $S_{u,\max}$ fitted Weibull growth function (blue) with a linear reduction during
4 deforestation (red shaded area) and mean 20-year return period root zone storage capacity S_R ,
5 20yr as equilibrium value for a) HJ Andrews WS1 with $a=0.0001 \text{ days}^{-1}$, $b=1.3$ and $S_{R, 20\text{yr}} =$
6 494 mm with b) the objective function values, c) Hubbard Brook WS2 with $a=0.001 \text{ days}^{-1}$,

1 $b=0.9$ and $S_{R, 20\text{yr}} = 22 \text{ mm}$ with d) the objective function values, and e) Hubbard Brook WS5
2 with $a=0.001 \text{ days}^{-1}$, $b=0.9$ and $S_{R, 20\text{yr}} = 49 \text{ mm}$ and with f) the objective function values.
3 The green shaded area represents the maximum and minimum boundaries of $S_{R,1\text{yr}}$ from the
4 water balance-based estimation, caused by the sampling of interception capacities.

5

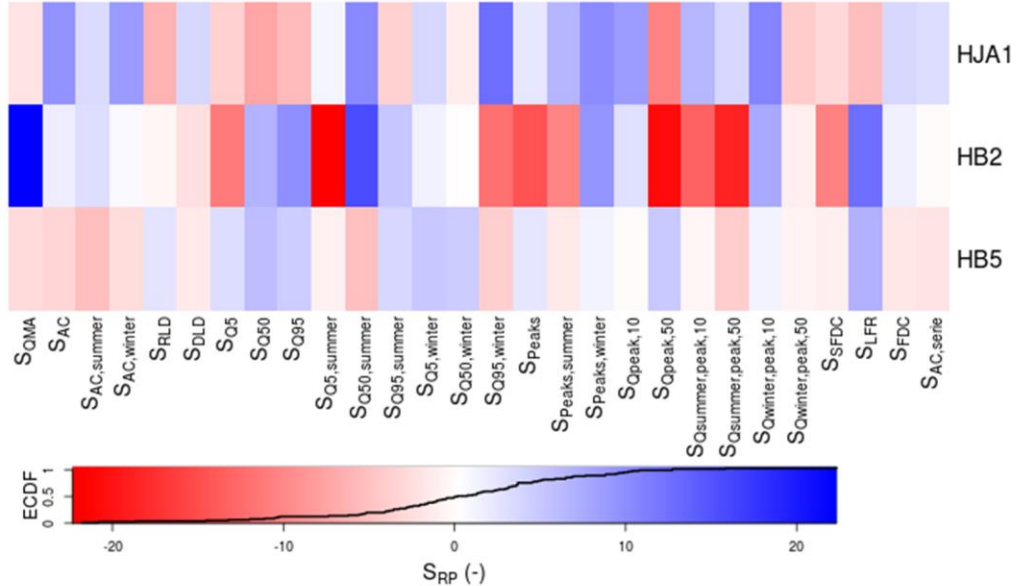
a)

dynamic - fixed



b)

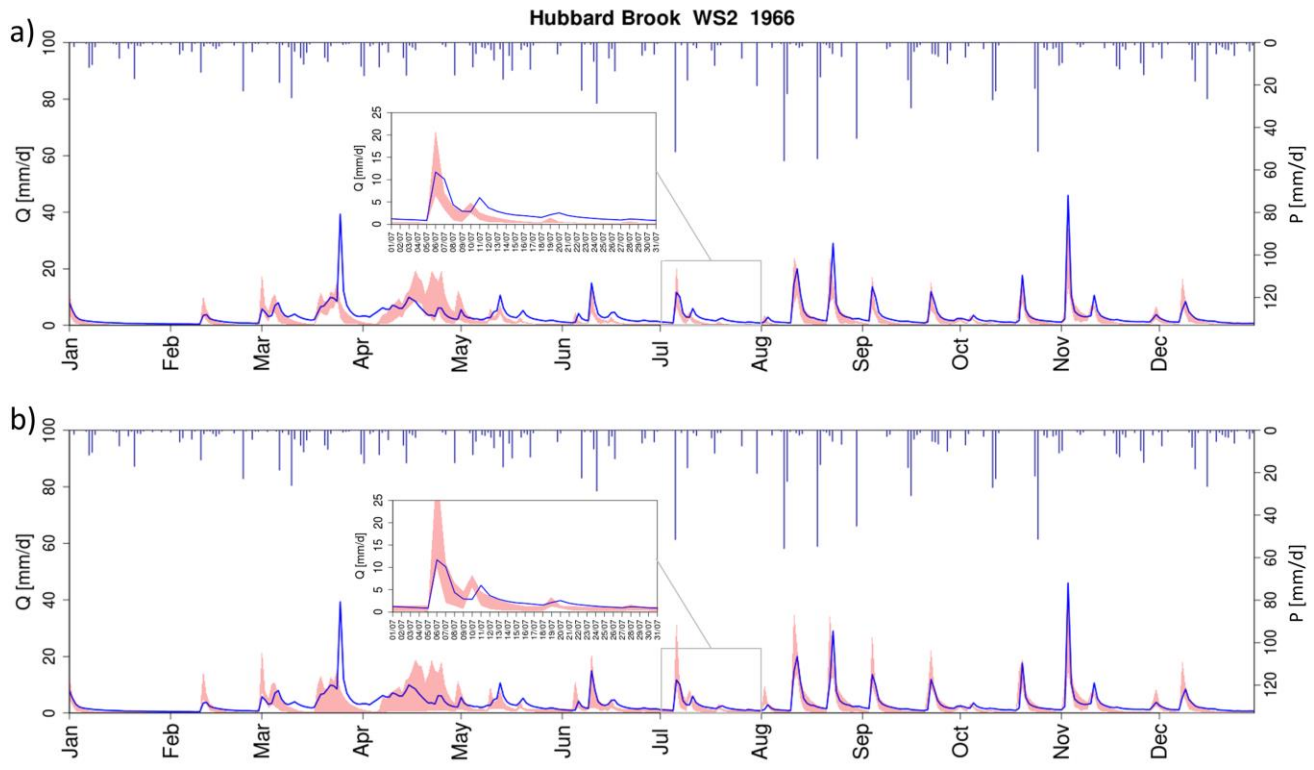
dynamic - fixed



1

2 Figure 9. Signature comparison between a time-dynamic and time-invariant formulation of
3 root zone storage capacity in the FLEX model with a) probabilities of improvement and b)
4 Ranked Probability Score for 28 hydrological signatures for HJ Andrews WS1 (HJA1),
5 Hubbard Brook WS2 (HB2) and Hubbard Brook WS5 (HB5). High values are shown in blue,
6 whereas a low values are shown in red.

7



1
2 Figure 10. Hydrograph of Hubbard Brook WS2 with the observed discharge (blue) and the
3 modelled discharge represented by the 5/ 95% uncertainty intervals (red), obtained with a) a
4 constant representation of the root zone storage capacity $S_{u,\max}$ and b) a time-varying
5 representation of the root zone storage capacity $S_{u,\max}$. Blue bars indicate precipitation.
6